Fluid Dyn. Res. **45** (2013) 055512 (30pp) doi:10.1088/0169-5983/45/5/055512

Weakly nonlinear sloshing in a truncated circular conical tank

I P Gavrilyuk[1], **M Hermann**[2], **I A Lukovsky**[3], **O V Solodun**[3] **and A N Timokha**[3,4]

[1] University of Cooperative Education, Eisenach D-99817, Germany
[2] Friedrich-Schiller-Universitaet Jena, D-07745 Jena Germany
[3] Institute of Mathematics, National Academy of Sciences of Ukraine, Kiev 01601, UKraine
[4] Department of Marine Technology, Norwegian University of Science and Technology, NO-7491 Trondheim, Norway

E-mail: alexander.timokha@ntnu.no

Received 23 March 2013, in final form 17 August 2013
Published 25 September 2013
Online at stacks.iop.org/FDR/45/055512

Communicated by M Funakoshi

Abstract
Sloshing of an ideal incompressible liquid in a rigid truncated (tapered) conical tank is considered when the tank performs small-magnitude oscillatory motions with the forcing frequency close to the lowest natural sloshing frequency. The multimodal method, the non-conformal mapping technique and the Moiseev type asymptotics are employed to derive a finite-dimensional system of weakly nonlinear ordinary differential (modal) equations. This modal system is a generalization of that by Gavrilyuk *et al* 2005 *Fluid Dyn. Res.* 37 399–429. Using the derived modal equations, we classify the resonant steady-state wave regimes occurring due to horizontal harmonic tank excitations. The frequency ranges are detected where the 'planar' and/or 'swirling' steady-state sloshing are stable as well as a range in which all steady-state wave regimes are not stable and irregular (chaotic) liquid motions occur is established. The results on the frequency ranges are qualitatively supported by experiments by Matta E 2002 *PhD Thesis* Politecnico di Torino, Torino.

(Some figures may appear in colour only in the online journal)

1. Introduction

The multimodal method is a rather popular analytically approximate approach to the nonlinear liquid sloshing problem. The method makes it possible to replace, in a rigorous mathematical way, the original free-boundary problem by a low-dimensional system of nonlinear ordinary differential equations (modal equations) and, thereby, it facilitates *analytical studies* of the

0169-5983/13/055512+30$33.00

contained liquid dynamics and associated hydrodynamic loads. Examples are reviewed in the books by Lukovsky (1990) and Faltinsen and Timokha (2009) as well as in Ikeda and Ibrahim (2005), Ikeda *et al* (2012), Takahara and Kimura (2012) and Lukovsky *et al* (2012). Along with the aforementioned low-dimensional modal systems providing analytical studies, the literature contains *computationally oriented* versions of the multimodal method. The latter versions deal with multi-dimensional modal systems of complex structure and relatively large dimension. Normally, they are used for simulating the transient sloshing. The computationally oriented modal equations are well represented by the fully nonlinear Perko's systems (see Moore and Perko 1964, Perko 1969, La Rocca *et al* 2000) and weakly nonlinear adaptive multimodal systems appearing in the papers by Faltinsen *et al* (2006, 2011), Limarchenko (2007), Love *et al* (2011), Love and Tait (2010, 2011).

The nonlinear multimodal method was originally proposed for tanks with vertical walls at the free surface. Using the non-conformal mapping technique by Lukovsky (1975) makes it possible to generalize the method for tanks with non-vertical walls. However, practical examples of the generalization are rare and almost fully represented by Lukovsky and Timokha (2002), Gavrilyuk *et al* (2005), Limarchenko (2007) and Faltinsen and Timokha (2013). A reason is that the multimodal method is rather sensitive to errors in satisfying the volume (mass) conservation condition, and, therefore, it is desirable to have analytically approximate natural sloshing modes which *exactly* satisfy the Laplace equation and the zero Neumann condition on the wetted tank walls. The required analytically approximate natural sloshing modes have been constructed for a non-truncated circular conical tank (Gavrilyuk *et al* 2005) and, recently, for a truncated circular conical tank (Gavrilyuk *et al* 2008). Bearing in mind that applications normally deal with truncated conical shapes, the constructed modes will be used in this paper to derive a seven-dimensional asymptotic nonlinear modal system of the Moiseev type which is, in fact, a generalization of that by Gavrilyuk *et al* (2005).

In section 2, we give differential and variational formulations of the problem. Applying the multimodal method combined with the non-conformal mapping technique yields a fully nonlinear infinite-dimensional (modal) system of nonlinear ordinary differential equations coupling the generalized coordinates and velocities. These equations are known for upright tanks as Perko-type modal equations (Moore and Perko 1964, Perko 1969, La Rocca *et al* 2000). Section 3 shortly outlines results by Gavrilyuk *et al* (2008) on the analytically approximate natural sloshing modes which are used in derivations of the Moiseev-type (Narimanov–Moiseev) asymptotic modal equations. In section 4, the latter equations are presented in an explicit form. Because derivation of these equations is a tedious analytical procedure with cumbersome formulae involved, the required technical details are reported in appendix A. Practically oriented readers do not need to follow computations of the appendix but, alternatively, may take the numerical non-dimensional hydrodynamic coefficients at nonlinear terms tabled for certain realistic tank proportions and liquid fillings. The hydrodynamic coefficients at the linear terms can be found in Gavrilyuk *et al* (2008, 2012).

The derived Moiseev type asymptotic modal equations are used to classify the steady-state resonant sloshing occurring due to a small-amplitude harmonic (horizontal or angular) tank excitation. The forcing frequency is close to the lowest natural sloshing frequency. In section 5, we construct an approximate time-periodic solution of the nonlinear modal equations which describes the steady-state wave regimes implying 'planar' and 'swirling' motions. Based on this solution, we study the possibility of secondary resonances. In contrast to Gavrilyuk *et al* (2005), these resonances depend on the two input parameters which can be interpreted as the semi-apex angle and the non-dimensional liquid depth. When a secondary resonance occurs, the Moiseev-type modal equations may be inapplicable. The first Lyapunov

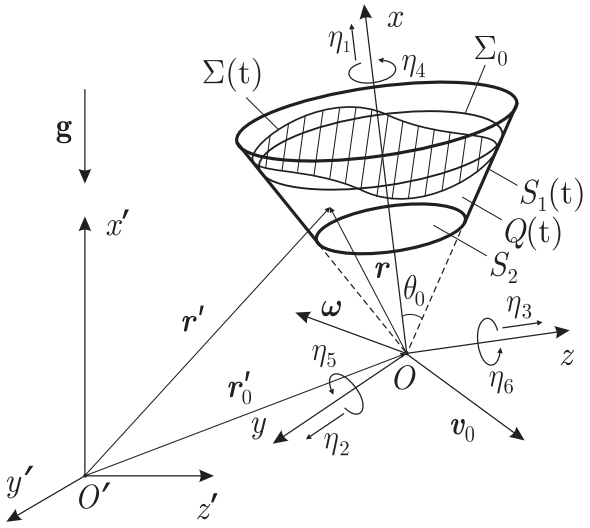

Figure 1. Sketch of the tapered conical container and adopted notations.

method is implemented in section 7 to distinguish stable and unstable steady-state wave regimes. We draw the response curves and detect the frequency ranges where the steady-state regimes are stable. The response curves are qualitatively similar to those reported by Gavrilyuk *et al* (2005) for a non-truncated conical tank. Along with the stability ranges for 'planar' and 'swirling', a frequency interval is indicated where irregular (chaotic) swirling may happen. The results on the frequency ranges are qualitatively supported by the model tests conducted by Matta (2002).

2. Statement of the problem

We consider a rigid truncated (tapered) conical tank of the semi-apex angle θ_0. The tank performs small-magnitude oscillatory motions with six degrees of freedom. These degrees are associated with translatory tank velocity $\boldsymbol{v}_0(t) = (\dot\eta_1, \dot\eta_2, \dot\eta_3)$ and the angular tank motions which could be defined by the instant angular velocity $\boldsymbol{\omega}(t) = (\dot\eta_4, \dot\eta_5, \dot\eta_6)$. The tank is partially filled by an ideal incompressible liquid performing an irrotational flow. The liquid motions as well as $\boldsymbol{v}_0(t)$ and $\boldsymbol{\omega}(t)$ are considered in the tank-fixed coordinate system $Oxyz$ whose origin O is superposed with the artificial cone vertex so that the Ox-axis coincides with the symmetry axis (figure 1). The gravity acceleration vector $\boldsymbol{g}$ has the opposite direction to $O'x'$.

2.1. Free-boundary problem

When introducing the absolute velocity potential $\Phi(x, y, z, t)$ defined in the $Oxyz$-coordinate system and function $\zeta(x, y, z, t)$ implicitly defining the free surface $\Sigma(t) : \zeta(x, y, z, t) = 0$, the free-boundary sloshing problem can be written in the form (see chapter 2 in Faltinsen and Timokha 2009)

$$\nabla^2\Phi = 0, \quad \boldsymbol{r} \in Q(t), \tag{1}$$

$$\frac{\partial\Phi}{\partial\nu} = \boldsymbol{v}_0 \cdot \boldsymbol{\nu} + \boldsymbol{\omega} \cdot (\boldsymbol{r} \times \boldsymbol{\nu}), \quad \boldsymbol{r} \in S(t), \tag{2}$$

$$\frac{\partial \Phi}{\partial \nu} = \boldsymbol{v}_0 \cdot \boldsymbol{\nu} + \boldsymbol{\omega} \cdot (\boldsymbol{r} \times \boldsymbol{\nu}) - \frac{\partial \zeta / \partial t}{|\nabla \zeta|}, \quad \boldsymbol{r} \in \Sigma(t), \tag{3}$$

$$\frac{\partial \Phi}{\partial t} + \frac{1}{2}|\nabla \Phi|^2 - \nabla \Phi \cdot (\boldsymbol{v}_0 + \boldsymbol{\omega} \times \boldsymbol{r}) + U = 0, \quad \boldsymbol{r} \in \Sigma(t), \tag{4}$$

$$\int_{Q(t)} \mathrm{d}Q = V_1 = \text{const}, \tag{5}$$

where $\boldsymbol{\nu}$ is the outer normal vector, $Q(t)$ is the liquid domain, $S(t) = S_1(t) \cup S_2$ is the wetted tank surface (S_2 is the tank bottom and $S_1(t)$ is the wetted tank walls), $\boldsymbol{r} = (x, y, z)$ is the radius vector, $U = \boldsymbol{r} \cdot \boldsymbol{g}$ is the gravity potential ($\boldsymbol{g}$ is the gravity acceleration vector). Equality (5) expresses the liquid volume V_1 conservation which is, in addition, the necessary solvability condition of the Neumann boundary problem (1)–(3).

The free-boundary problem (1)–(5) needs initial conditions determining the instant free-surface pattern and the normal velocity on $\Sigma(t)$ at $t = t_0$, i.e. $\zeta(x, y, z, t_0) = \zeta_0(x, y, z)$, $\partial \Phi / \partial \nu|_{\Sigma(t_0)} = \Phi_0(x, y, z)|_{\Sigma(t_0)}$, where $\zeta_0(x, y, z)$ and $\Phi_0(x, y, z)|_{\Sigma(t_0)}$ are the two known functions. For the steady-state wave solutions, the periodicity condition should be adopted.

2.2. The Bateman–Luke formulation

Instead of dealing with the free-boundary problem (1)–(5), the multimodal method normally employs the Bateman–Luke variational formulation whose equivalence to the original free surface problem is, for instance, proved in section 2.5.3.2 by Faltinsen and Timokha (2009) and in chapter 2 by Lukovsky and Timokha (1995). According to this formulation, the solution (Φ and ζ) coincides with the extrema points of the action

$$A(\zeta, \Phi) = \int_{t_1}^{t_2} \left(\int_{Q(t)} [p - p_0] \, \mathrm{d}x \, \mathrm{d}y \, \mathrm{d}z \right) \mathrm{d}t \tag{6}$$

for arbitrary t_1 and t_2 ($t_1 < t_2$) subject to the variations satisfying

$$\delta \Phi|_{t_1, t_2} = 0, \quad \delta \zeta|_{t_1, t_2} = 0. \tag{7}$$

The pressure field $p(x, y, z, t)$ can be determined by using the Bernoulli equation rewritten in the non-inertial coordinate system $Oxyz$ as follows:

$$\frac{\partial \Phi}{\partial t} + \frac{1}{2}|\nabla \Phi|^2 - \nabla \Phi \cdot (\boldsymbol{v}_0 + \boldsymbol{\omega} \times \boldsymbol{r}) + U = -\frac{p - p_0}{\rho}, \tag{8}$$

where p_0 is the ullage pressure and ρ is the liquid density.

2.3. General modal equations

The Bateman–Luke variational formulation was extensively used by many authors to derive nonlinear modal equations for *upright tanks* (the tanks having vertical walls at the free surface) when the single-valued presentation of $\Sigma(t)$: $\zeta = x - f(y, z, t) = 0$ is possible. The derivation assumed that f is expanded in a Fourier series with the time-dependent coefficients $\{\beta_N(t)\}$ playing the role of *the generalized coordinates*. For non-vertical walls, the Fourier representation is impossible and, therefore, we have to introduce the generalized

coordinates implicitly

$$\zeta = \zeta(x, y, z; \{\beta_N(t)\}) \tag{9}$$

subject to the volume conservation condition (5) considered as a holonomic constraint.

We introduce the modal representation of the velocity potential

$$\Phi(x, y, z, t) = \boldsymbol{v}_0 \cdot \boldsymbol{r} + \boldsymbol{\omega} \cdot \boldsymbol{\Omega}(x, y, z, \{\beta_N(t)\}) + \sum_{N=1}^{\infty} F_N(t)\varphi_N(x, y, z), \tag{10}$$

where $\{\varphi_N\}$ is a complete set of linearly independent harmonic functions defined in $Q(t)$ for any admissible instant liquid shapes, $\boldsymbol{\Omega} = (\Omega_1, \Omega_2, \Omega_3)$ are the Stokes–Joukowski potentials which are parametrically dependent functions of β_N as being the solution of the Neumann boundary value problem

$$\nabla^2\Omega_i = 0 \text{ in } Q(t), \quad \frac{\partial\Omega_1}{\partial\nu} = y\nu_z - z\nu_y, \quad \frac{\partial\Omega_2}{\partial\nu} = z\nu_x - x\nu_z,$$
$$\frac{\partial\Omega_3}{\partial\nu} = x\nu_y - y\nu_x \quad \text{on} \quad \Sigma(t) \cup S(t). \tag{11}$$

Here, ν_i are the projections of the outer normal on the coordinate axes and $\{F_N(t)\}$ play the role of the *generalized velocities*. The Fourier-type solution (10) should keep the volume (mass) conservation that requires $\{\varphi_N\}$ to *exactly satisfy* the Laplace equation and the zero-Neumann boundary condition on the wetted tank surface.

Because ζ and Φ are independent variables in the Bateman–Luke formulation, the generalized coordinates $\{\beta_N\}$ and velocities $\{F_N\}$ are also independent and, due to (7), satisfy the condition $\delta F_N|_{t=t_1,t_2} = \delta\beta_N|_{t=t_1,t_2} = 0$. Substituting (10) into (6) and varying F_N (Faltinsen and Timokha (2009), chapter 5) leads to the kinematic modal equations

$$\frac{\mathrm{d}A_N}{\mathrm{d}t} \equiv \sum_K \frac{\partial A_N}{\partial\beta_K}\dot{\beta}_K = \sum_K A_{NK}F_K \quad \text{for all } N. \tag{12}$$

Following the derivations in (Faltinsen and Timokha (2009), pp 301–3) leads to the dynamic modal equations

$$\sum_K \frac{\partial A_K}{\partial\beta_N}\dot{F}_K + \frac{1}{2}\sum_{K,L}\frac{\partial A_{KL}}{\partial\beta_N}F_KF_L + (\boldsymbol{\omega}\times\boldsymbol{v}_0 - \boldsymbol{g})\cdot\frac{\partial\boldsymbol{l}}{\partial\beta_i} - \frac{1}{2}\boldsymbol{\omega}\cdot\frac{\partial\boldsymbol{J}^1}{\partial\beta_i}\cdot\boldsymbol{\omega}$$
$$+\dot{\boldsymbol{\omega}}\cdot\left(\frac{\partial\boldsymbol{l}_\omega}{\partial\beta_i} - \frac{\partial\boldsymbol{l}_{\omega t}}{\partial\dot{\beta}_i}\right) + \boldsymbol{\omega}\left(\frac{\partial\boldsymbol{l}_{\omega t}}{\partial\beta_i} - \frac{\mathrm{d}}{\mathrm{d}t}\frac{\partial\boldsymbol{l}_{\omega t}}{\partial\dot{\beta}_i}\right) = 0 \quad \text{for all } N. \tag{13}$$

The modal equations (12) and (13) are formulated with respect to the aforementioned generalized coordinates and velocities, where

$$A_N = \int_{Q(t)}\varphi_N\,\mathrm{d}Q, \quad A_{NK} = \int_{Q(t)}(\nabla\varphi_N\cdot\nabla\varphi_K)\,\mathrm{d}Q,$$
$$l_1 = \int_{Q(t)}x\,\mathrm{d}Q, \quad l_2 = \int_{Q(t)}y\,\mathrm{d}Q, \quad l_3 = \int_{Q(t)}z\,\mathrm{d}Q, \tag{14}$$
$$l_{k\omega} = \rho\int_{Q(t)}\Omega_k\,\mathrm{d}Q, \; l_{k\omega t} = \rho\int_{Q(t)}\frac{\partial\Omega_k}{\partial t}\,\mathrm{d}Q, \; J^1_{ij} = \rho\int_{S(t)+\Sigma(t)}\Omega_i\frac{\partial\Omega_j}{\partial t}\,\mathrm{d}Q,$$

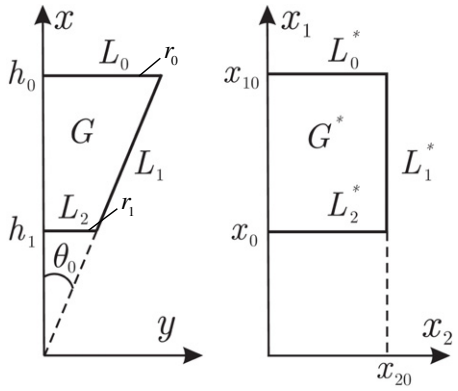

Figure 2. The physical and transformed meridional cross-sections.

$J^1_{ij} = J^1_{ji}$, $i, j, k = 1, 2, 3$ are implicitly defined nonlinear functions of generalized coordinates β_N (the time evolution of $Q(t)$ is fully determined by (9)). Here, $\boldsymbol{J}^1$ is the inertia tensor of the contained liquid, $\boldsymbol{l}/V_1$ is the dynamic liquid mass center, but the vectors $\boldsymbol{l}_\omega$ and $\boldsymbol{l}_{\omega t}$ have no a clear physical interpretation.

3. Analytically approximate natural sloshing modes

Normally, the functional set $\{\varphi_N\}$ in (10) is associated with the natural sloshing modes which are the eigenfunctions of the spectral boundary problem

$$\nabla^2\varphi = 0, \quad \boldsymbol{r} \in Q_0, \quad \frac{\partial\varphi}{\partial\nu} = 0, \quad \boldsymbol{r} \in S_0, \quad \frac{\partial\varphi}{\partial\nu} = \bar{\kappa}\varphi, \quad \boldsymbol{r} \in \Sigma_0, \quad \int_{\Sigma_0} \frac{\partial\varphi}{\partial\nu}\mathrm{d}S = 0 \tag{15}$$

formulated in the hydrostatic (mean) liquid domain Q_0 bounded by the hydrostatic free surface Σ_0 and the mean wetted tank surface S_0.

A mathematical inconsistency is that the natural sloshing modes are defined in the unperturbed domain Q_0 but, to make the integrals (14) mathematically correct, the multimodal method requires the eigensolution of (15) which is expandable over Σ_0 into the 'ullage' domain. Another important limitation is that the modal solution should be as precise as to satisfy the mass (volume) conservation and, therefore, the functional set $\{\varphi_N\}$ must be harmonic functions satisfying the zero-Neumann condition on the wetted tank surface.

To get an explicit definition of (9), we employ the non-conformal mapping technique by introducing the curvilinear coordinate system $Ox_1x_2x_3$

$$x = x_1, \quad y = x_1x_2\cos x_3, \quad z = x_1x_2\sin x_3 \tag{16}$$

($x_3 = \eta$ is the angular coordinate) transforming the conical domain to the circular cylindrical shape as demonstrated in figure 2 for the meridional cross-section of the static (mean) liquid domain in the physical G and transformed G^* planes. Considering the eigensolution of (15) in the curvilinear coordinate system

$$\varphi(x_1, x_2, x_3) = \psi_m(x_1, x_2)\begin{matrix}\sin m\,x_3\\ \cos m\,x_3\end{matrix}, \quad m = 0, 1, 2, \ldots \tag{17}$$

makes it possible to separate the spatial variables (x_1, x_2) and x_3 so that one yields the following m-family of spectral boundary problems:

$$p\frac{\partial^2\psi_m}{\partial x_1^2}+2q\frac{\partial^2\psi_m}{\partial x_1\partial x_2}+s\frac{\partial^2\psi_m}{\partial x_2^2}+d\frac{\partial\psi_m}{\partial x_2}-m^2c\psi_m=0 \quad \text{in} \quad G^*, \tag{18}$$

$$s\frac{\partial\psi_m}{\partial x_2}+q\frac{\partial\psi_m}{\partial x_1}=0 \quad \text{on} \quad L_1^*, \tag{19}$$

$$p\frac{\partial\psi_m}{\partial x_1}+q\frac{\partial\psi_m}{\partial x_2}=\bar{\kappa}_m p\psi_m \quad \text{on} \quad L_0^*, \tag{20}$$

$$p\frac{\partial\psi_m}{\partial x_1}+q\frac{\partial\psi_m}{\partial x_2}=0 \quad \text{on} \quad L_2^*, \tag{21}$$

$$|\psi_m(x_1,0)|<\infty, \quad m=0,1,2,\ldots, \tag{22}$$

$$\int_0^{x_{20}}\psi_0 x_2\,\mathrm{d}x_2=0, \tag{23}$$

where $G^*=\{(x_1,x_2): x_0\leqslant x_1\leqslant x_{10},\ 0\leqslant x_2\leqslant x_{20}\}$, $p=x_1^2x_2$, $q=-x_1x_2^2$, $s=x_2(x_2^2+1)$, $d=1+2x_2^2$, $c=1/x_2$ and L_0^*, L_1^* and L_2^* are defined in figure 2. The natural sloshing frequencies are

$$\sigma_{mn}=\sqrt{g\bar{\kappa}_{mn}}=\sqrt{\frac{g\kappa_{mn}}{r_0}}, \tag{24}$$

where $\kappa_{mn}=r_0\bar{\kappa}_{mn}$ are the non-dimensional eigenvalues normalized by the mean free surface radius r_0. The lowest natural sloshing frequency is associated with κ_{11}. Dependences of the non-dimensional spectral parameters κ_{mn} on the lower-to-upper radii $\mathtt{r}_1=r_1/r_0$ (see figure 2) are extensively discussed by Gavrilyuk *et al* (2008).

By using the Trefftz method, Gavrilyuk *et al* (2008) constructed the required analytically approximate Trefftz solution of (18)–(23) which exactly satisfies (18), (19) and (21)

$$\psi_m=\psi_{mn}(x_1,x_2)=\sum_{k=1}^{q_1}a_{n,k}^{(m)}w_k^{(m)}+\sum_{l=1}^{q_2}\bar{a}_{n,l}^{(m)}\bar{w}_l^{(m)}, \tag{25}$$

where $w_k^{(m)}(x_1,x_2)=N_k^{(m)}\,x_1^{\nu_{mk}}\,T_{\nu_{mk}}^{(m)}(x_2)$, $\bar{w}_k^{(m)}(x_1,x_2)=\bar{N}_k^{(m)}\,x_1^{-1-\nu_{mk}}\,\bar{T}_{\nu_{mk}}^{(m)}(x_2)$ with $T_{\nu_{mk}}^{(m)}(x_2)$ and $\bar{T}_{\nu_{mk}}^{(m)}(x_2)$ expressed via the associate Legendre polynomials of the first kind, $P_\nu^{(m)}(\mu)$, as follows:

$$T_{\nu_{mk}}^{(m)}(x_2)=(1+x_2^2)^{\frac{\nu_{mk}}{2}}P_{\nu_{mk}}^{(m)}\left(\frac{1}{\sqrt{1+x_2^2}}\right), \quad \bar{T}_{\nu_{mk}}^{(m)}(x_2)=(1+x_2^2)^{\frac{-1-\nu_{mk}}{2}}P_{\nu_{mk}}^{(m)}\left(\frac{1}{\sqrt{1+x_2^2}}\right).$$

The numbers ν_{mk} are the roots of $\partial P_\nu^{(m)}(\cos\theta)/\partial\theta|_{\theta=\theta_0}=0$ and $N_k^{(m)}$ and $\bar{N}_k^{(m)}$ are the normalizing multipliers introduced to satisfy the condition $||w_k^{(m)}||^2_{L_2^*\cup L_0^*}=||\bar{w}_k^{(m)}||^2_{L_2^*\cup L_0^*}=1$, where $||\cdot||$ implies the mean square-root norm on $L_2^*\cup L_0^*$.

4. Weakly nonlinear modal equations

4.1. Modal solution

We consider (9) in the $x_1x_2x_3$-coordinates, i.e. $\zeta = \zeta(x_1, x_2, x_3, \{\beta_{mi}\})$, and postulate it as

$$\zeta = x_1 - f(x_2, x_3, t) = x_1 - f(x_2, x_3, \{p_{mi}\},$$
$$\{r_{mi}\}) = x_1 - x_{10} - \beta_0(t) - \sum_{m=0}^{\infty}\sum_{i=1}^{\infty}(p_{mi}(t)\cos(mx_3) + r_{mi}(t)\sin(mx_3))\, f_{mi}(x_2), \tag{26}$$

where x_{10} is the distance between the origin and the mean free surface (see figure 2) and

$$f_{mi}(x_2) = \frac{\sigma_{mi}}{g}\psi_{mi}(x_{10}, x_2) \tag{27}$$

defines the radial natural surface profiles and σ_{mi} are the natural sloshing frequencies by (24). Satisfying the volume conservation condition (5) makes $\beta_0(t)$ a function of other generalized coordinates, $\beta_0 = G(\{p_{mi}\}, \{r_{mi}\})$.

The modal representation of the velocity potential (10) takes the form

$$\Phi(x_1, x_2, x_3, t) = \boldsymbol{v}_0 \cdot \boldsymbol{r} + \boldsymbol{\omega} \cdot \boldsymbol{\Omega} + \sum_{m=0}^{\infty}\sum_{i=1}^{\infty}\Big(P_{mi}(t)\cos(mx_3) + R_{mi}(t)\sin(mx_3)\Big)\psi_{mi}(x_1, x_2). \tag{28}$$

According to (26) and (28), integrals (14) are fully determined by the generalized coordinates $\{p_{mi}\}$ and $\{r_{mi}\}$ in which the capital indices should be replaced by the complex indices $(mi, \cos)$ and $(mi, \sin)$ so that, for instance, when $N = (mi, \cos)$,

$$A_N = A_{(mi,\cos)} = \int_{-\pi}^{\pi}\int_{0}^{r_0}\int_{x_0}^{f(x_2,x_3,\{p_{mi}\},\{r_{mi}\})} x_1^2 x_2 \psi_{mi}(x_1, x_2)\cos(mx_3)\,\mathrm{d}x_1\,\mathrm{d}x_2\,\mathrm{d}x_3.$$

4.2. The Moiseev asymptotics

Henceforth, we assume that the problem is scaled by the mean free surface radius so that all geometric parameters and generalized coordinates are non-dimensional and, of course, the circle Σ_0 has the unit radius. The ratio between the bottom and free-surface radii is denoted by $\mathtt{r}_1 = r_1/r_0$.

We adopt the Moiseev asymptotics (Narimanov 1957, Moiseev 1958, Lukovsky *et al* 2012) for the introduced generalized coordinates and velocities. This asymptotics holds true for resonant tank excitations with the mean forcing frequency close to the lowest natural sloshing frequency and the secondary resonances are neglected. The Moiseev asymptotics has been widely used in the papers on the multimodal method (Faltinsen *et al* 2000, Gavrilyuk *et al* 2005, 2007, Ikeda and Ibrahim 2005, Lukovsky *et al* 2012, Takahara and Kimura 2012, Faltinsen and Timokha 2013) as well as in other semi-analytical approaches to the nonlinear sloshing problem with a finite liquid depth (Ockendon and Ockendon 1973, Bridges 1986, 1987, Waterhouse 1994, Ockendon *et al* 1996).

The Moiseev asymptotics suggests that the non-dimensional forcing magnitude is of the order $\epsilon \ll 1$. For axisymmetric tanks, this causes the two primary excited lowest modes, differing only by the $\pi/2$-azimuthal angle, and associated with the non-dimensional generalized coordinates p_{11} and r_{11} to dominate. These are of the order $O(\epsilon^{1/3})$. A simple

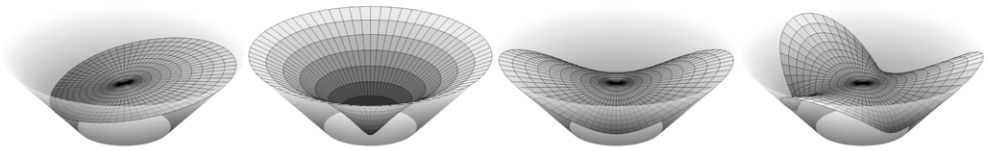

Figure 3. Wave patterns associated with the generalized coordinates included into our nonlinear modal analysis. Except for p_{01}, these patterns appear twice differing by $\pi/2$-azimuthal rotation. The drawings for $\theta_0 = 30^\circ$ and the non-dimensional ratio of the lower (bottom) and upper (the mean free surface) radii is $\mathtt{r_1} = 0.5$.

trigonometric analysis by the angular coordinate leads to the following asymptotic relations for the generalized coordinates and velocities:

$$\frac{P_{11}}{\sigma_{11}} \sim \frac{R_{11}}{\sigma_{11}} \sim p_{11} \sim r_{11} = O(\epsilon^{1/3}), \quad \frac{P_{2n}}{\sigma_{2n}} \sim \frac{R_{2n}}{\sigma_{2n}} \sim \frac{P_{0n}}{\sigma_{0n}} \sim p_{2n} \sim r_{2n} \sim p_{0n} = O(\epsilon^{2/3}),$$

$$\frac{P_{3n}}{\sigma_{3n}} \sim \frac{R_{3n}}{\sigma_{3n}} \sim \frac{P_{1(n+1)}}{\sigma_{1(n+1)}} \sim \frac{R_{1(n+1)}}{\sigma_{1(n+1)}} \sim p_{3n} \sim r_{3n} \sim p_{1(n+1)} \sim r_{1(n+1)} = O(\epsilon), \quad n \geqslant 1. \tag{29}$$

Remaining non-dimensional generalized coordinates and velocities are of the order $o(\epsilon)$ and can be neglected within the framework of the Moiseev asymptotics.

4.3. Finite-dimensional asymptotic modal equations

Derivation of asymptotic modal systems based on the Moiseev asymptotics (29) implies neglecting the $o(\epsilon)$-order terms in the modal equations (12) and (13). As a consequence, we arrive at an infinite-dimensional system of nonlinear ordinary differential equations with respect to the generalized coordinates and velocities (29). Examples of such infinite-dimensional systems are given by Lukovsky *et al* (2012) and Faltinsen and Timokha (2013). Other existing asymptotic analytically oriented modal equations, e.g. in Lukovsky (1990), Gavrilyuk *et al* (2005), involve two dominant, r_{11} and p_{11}, and three second-order generalized coordinates and velocities associated with p_{01}, p_{21} and r_{21}. Faltinsen and Timokha (2009) showed that these five-dimensional nonlinear modal equations enable an accurate approximation of the steady-state sloshing due to resonant excitations of the lowest natural modes. This means that the weakly nonlinear modal equations of the Moiseev type do not require to include a large set of generalized coordinates of the second and third order. A physical reason for that is that the major of kinematic energy is normally accumulated by the natural sloshing modes possessing the lower natural sloshing frequencies.

For an upright circular cylindrical tank, it was enough to account for three second-order generalized coordinates associated with p_{01}, p_{21} and r_{21} in addition to the two dominant generalized coordinates r_{11} and p_{11}. Based on this fact, we include in our modal analysis the aforementioned five lowest modes associated with and, in addition, the two third-order generalized coordinates p_{31} and r_{31}. The wave patterns of the adopted natural sloshing modes are shown in figure 3.

Technical derivation details for the seven-dimensional Moiseev-type modal system are outlined in appendix A. For brevity, the generalized coordinates and velocities are

denoted as follows:

$$p_{01}=p_0,\quad r_{11}=r_1,\quad p_{11}=p_1,\quad r_{21}=r_2,\quad p_{21}=p_2,\quad r_{31}=r_3,\quad p_{31}=p_3,$$
$$P_{01}=P_0,\quad R_{11}=R_1,\quad P_{11}=P_1,\quad R_{21}=R_2,\quad P_{21}=P_2,\quad R_{31}=R_3,\quad P_{31}=P_3.$$

The result is the following system of ordinary differential equations coupling the non-dimensional generalized coordinates:

$$\ddot{p}_0+\sigma_0^2 p_0+\mathtt{d}_8(\dot{p}_1^2+\dot{r}_1^2)+\mathtt{d}_{10}(\ddot{p}_1 p_1+\ddot{r}_1 r_1)+\sigma_0^2\mathtt{g}_0(p_1^2+r_1^2)=0, \tag{30}$$

$$\begin{aligned}\ddot{r}_1+\sigma_1^2 r_1+\mathtt{d}_1 r_1(\ddot{p}_1 p_1+\ddot{r}_1 r_1+\dot{p}_1^2+\dot{r}_1^2)+\mathtt{d}_2(p_1(\ddot{r}_1 p_1-\ddot{p}_1 r_1)+2\dot{p}_1(\dot{r}_1 p_1-\dot{p}_1 r_1))\\ +\mathtt{d}_3(\ddot{p}_1 r_2-\ddot{r}_1 p_2+\dot{p}_1\dot{r}_2-\dot{p}_2\dot{r}_1)+\mathtt{d}_4(\ddot{r}_2 p_1-\ddot{p}_2 r_1)+\mathtt{d}_5(\ddot{r}_1 p_0+\dot{r}_1\dot{p}_0)+\mathtt{d}_6\ddot{p}_0 r_1\\ +\sigma_1^2(\mathtt{g}_1 p_0 r_1+\mathtt{g}_2(p_1 r_2-p_2 r_1)+\mathtt{g}_3(p_1^2+r_1^2)r_1)+\Lambda(\dot{v}_{03}+g\theta_2)=0,\end{aligned} \tag{31}$$

$$\begin{aligned}\ddot{p}_1+\sigma_1^2 p_1+\mathtt{d}_1 p_1(\ddot{p}_1 p_1+\ddot{r}_1 r_1+\dot{p}_1^2+\dot{r}_1^2)+\mathtt{d}_2(r_1(\ddot{p}_1 r_1-\ddot{r}_1 p_1)+2\dot{r}_1(\dot{p}_1 r_1-\dot{r}_1 p_1))\\ +\mathtt{d}_3(\ddot{p}_1 p_2+\ddot{r}_1 r_2+\dot{p}_1\dot{p}_2+\dot{r}_1\dot{r}_2)+\mathtt{d}_4(\ddot{p}_2 p_1+\ddot{r}_2 r_1)+\mathtt{d}_5(\ddot{p}_1 p_0+\dot{p}_1\dot{p}_0)+\mathtt{d}_6\ddot{p}_0 p_1\\ +\sigma_1^2(\mathtt{g}_1 p_0 p_1+\mathtt{g}_2(p_1 p_2+r_1 r_2)+\mathtt{g}_3(p_1^2+r_1^2)p_1)+\Lambda(\dot{v}_{02}-g\theta_3)=0,\end{aligned} \tag{32}$$

$$\ddot{r}_2+\sigma_2^2 r_2+2\mathtt{d}_7\dot{p}_1\dot{r}_1+\mathtt{d}_9(\ddot{p}_1 r_1+\ddot{r}_1 p_1)+2\sigma_2^2\mathtt{g}_4 p_1 r_1=0, \tag{33}$$

$$\ddot{p}_2+\sigma_2^2 p_2+\mathtt{d}_7(\dot{p}_1^2-\dot{r}_1^2)+\mathtt{d}_9(\ddot{p}_1 p_1-\ddot{r}_1 r_1)+\sigma_2^2\mathtt{g}_4(p_1^2-r_1^2)=0, \tag{34}$$

$$\begin{aligned}\ddot{r}_3+\sigma_3^2 r_3+\mathtt{d}_{11}(\ddot{r}_1(p_1^2-r_1^2)+2\ddot{p}_1 p_1 r_1)+\mathtt{d}_{12}(r_1(\dot{p}_1^2-\dot{r}_1^2)+2\dot{p}_1\dot{r}_1 p_1)+\mathtt{d}_{13}(\ddot{p}_1 r_2+\ddot{r}_1 p_2)\\ +\mathtt{d}_{14}(\ddot{p}_2 r_1+\ddot{r}_2 p_1)+\mathtt{d}_{15}(\dot{p}_1\dot{r}_2+\dot{p}_2\dot{r}_1)+\sigma_3^2(\mathtt{g}_5(p_1 r_2+p_2 r_1)\\ +\mathtt{g}_6 r_1(3p_1^2-r_1^2))=0,\end{aligned} \tag{35}$$

$$\begin{aligned}\ddot{p}_3+\sigma_3^2 p_3+\mathtt{d}_{11}(\ddot{p}_1(p_1^2-r_1^2)-2\ddot{r}_1 p_1 r_1)+\mathtt{d}_{12}(p_1(\dot{p}_1^2-\dot{r}_1^2)-2\dot{p}_1\dot{r}_1 r_1)+\mathtt{d}_{13}(\ddot{p}_1 p_2-\ddot{r}_1 r_2)\\ +\mathtt{d}_{14}(\ddot{p}_2 p_1-\ddot{r}_2 r_1)+\mathtt{d}_{15}(\dot{p}_1\dot{p}_2-\dot{r}_1\dot{r}_2)+\sigma_3^2(\mathtt{g}_5(p_1 p_2-r_1 r_2)\\ +\mathtt{g}_6 p_1(p_1^2-3r_1^2))=0.\end{aligned} \tag{36}$$

Here, the non-dimensional hydrodynamic coefficients are functions of the mean liquid domain parameters; the corresponding formulae for them are given in appendix A. The natural sloshing frequencies $\sigma_i=\sigma_{i1}$ are defined by (24) where κ_{m1} are the corresponding non-dimensional eigenvalues whose numerical values (as well as those for Λ) can be found in Gavrilyuk *et al* (2008, 2012).

4.4. Non-dimensional hydrodynamic coefficients

Whereas $\mathtt{r}_1\to 0$, the tank becomes non-truncated and, as expected, the non-dimensional hydrodynamic coefficients tend to the numerical values by Gavrilyuk *et al* (2005). For another limit case $\theta_0\to 0$, the tank tends to the upright circular cylindrical shape and modal equations (30)–(36) should transform to the corresponding seven modal equations taken from the infinite-dimensional modal system by Lukovsky *et al* (2012).

Figures 4 and 5 illustrate how the non-dimensional hydrodynamic coefficients $\mathtt{d}_\mathtt{i}$ and $\mathtt{g}_\mathtt{j}$ depend on $0<\theta_0<45^\circ$ for the fixed non-dimensional liquid depth $h=1$. The limit values

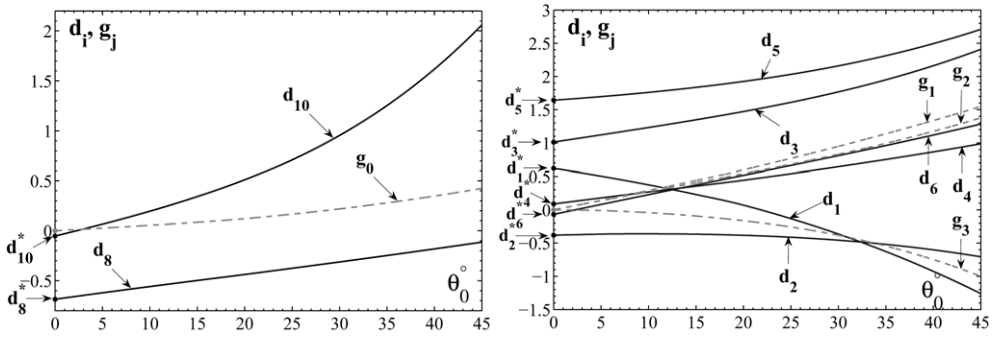

Figure 4. Coefficients $\mathtt{d}_i$, $i = 1, \ldots, 6$, $\mathtt{d}_8$, $\mathtt{d}_{10}$ and $\mathtt{g}_i$, $i = 0, 1, 2, 3$ as functions of θ_0 for the non-dimensional depth $h = 1$.

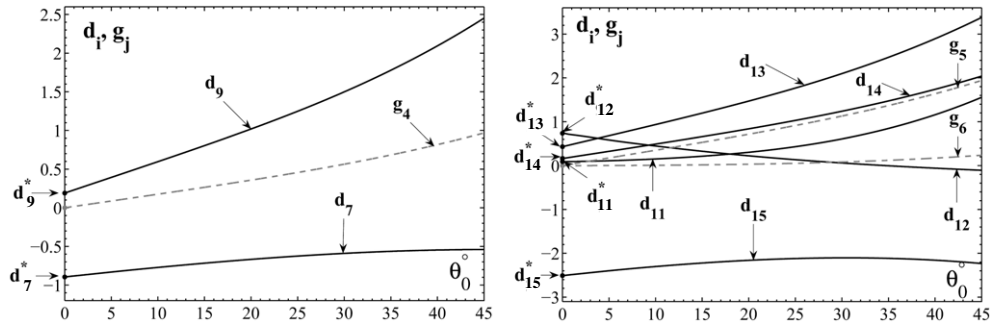

Figure 5. Coefficients $\mathtt{d}_7$, $\mathtt{d}_9$, $\mathtt{d}_i$, $i = 11, \ldots, 15$, and $\mathtt{g}_i$, $i = 4, 5, 6$ as functions of θ_0 for the non-dimensional depth $h = 1$.

on the vertical axis ($\theta_0 = 0$) coincide with the coefficients in the front of the corresponding nonlinear terms computed for an upright circular cylindrical tank which were calculated by using the exact natural sloshing modes (Lukovsky *et al* 2012). The limit values are marked by $\mathtt{d}_i^*$.

The modal equations (30)–(36) contain the hydrodynamic coefficients $\mathtt{g}_j$ which are not zero only for tanks with non-vertical walls. The graphs confirm that the limit numerical values $\mathtt{g}_j$ tend to zero when the semi-apex angle tends to zero.

Tables 1–3 present the numerical non-dimensional hydrodynamic coefficients $\mathtt{d}_i$ and $\mathtt{g}_j$ ($m = 0, 1, 2, 3$, $i = 1, \ldots, 15$, $j = 0, \ldots, 6$) for three semi-angles, but κ_m and Λ can be found in Gavrilyuk *et al* (2008, 2012).

The hydrodynamic coefficients of the modal equations can be rewritten in the dimensional form using the formulae

$$\bar{\mathtt{d}}_i = \begin{cases} \mathtt{r}_0\,\mathtt{d}_i, & \text{for } i = 1, 2, 9, 10, \\ \mathtt{r}_0^2\,\mathtt{d}_i, & \text{for } i = 3, \ldots, 8, 11, \ldots, 15, \end{cases} \qquad \bar{\mathtt{g}}_i = \begin{cases} \mathtt{r}_0\,\mathtt{g}_i, & \text{for } i = 0, 1, 2, 4, 5, \\ \mathtt{r}_0^2\,\mathtt{g}_i, & \text{for } i = 3, 6. \end{cases} \tag{37}$$

5. The time-periodic solution of the modal equations

We consider forced steady-state resonant liquid sloshing occurring due to harmonic translatory tank excitations. For brevity, the excitations are assumed along the Oz-axis in notations of figure 1 implying that $\eta_i = 0$, $i \neq 3$ and $\eta_3 = H\cos(\sigma t)$. Our task consists of

Table 1. Non-dimensional hydrodynamic coefficients $\mathtt{d_i}$ ($i = 1, \ldots, 8$) computed within the five significant figures.

$\mathtt{r_1}$	$\mathtt{d_1}$	$\mathtt{d_2}$	$\mathtt{d_3}$	$\mathtt{d_4}$	$\mathtt{d_5}$	$\mathtt{d_6}$	$\mathtt{d_7}$	$\mathtt{d_8}$
$\theta_0 = 30^\circ$								
0.0	−0.317 55	−0.453 74	1.7656	0.635 50	2.1563	0.811 79	−0.581 51	−0.310 82
0.1	−0.317 55	−0.453 74	1.7656	0.635 50	2.1563	0.811 79	−0.581 51	−0.310 83
0.2	−0.317 54	−0.453 74	1.7656	0.635 48	2.1563	0.811 77	−0.581 55	−0.310 85
0.3	−0.317 33	−0.453 59	1.7656	0.635 24	2.1563	0.811 42	−0.582 24	−0.311 39
0.4	−0.315 75	−0.452 51	1.7651	0.633 47	2.1564	0.808 79	−0.587 34	−0.315 38
0.5	−0.308 11	−0.447 26	1.7629	0.625 29	2.1573	0.796 78	−0.611 14	−0.333 93
0.6	−0.278 06	−0.426 57	1.7573	0.597 33	2.1633	0.756 89	−0.695 95	−0.400 16
0.7	−0.160 37	−0.345 23	1.7530	0.519 23	2.2053	0.653 10	−0.960 10	−0.607 74
0.8	0.390 82	0.040 81	1.7969	0.319 93	2.4525	0.424 26	−1.7657	−1.2405
0.9	4.6122	3.0301	2.1361	−0.312 00	3.7413	−0.212 07	−4.6357	−3.3619
$\theta_0 = 45^\circ$								
0.0	−1.2608	−0.706 38	2.4092	0.987 22	2.7093	1.2837	−0.540 21	−0.113 91
0.1	−1.2608	−0.706 38	2.4092	0.987 20	2.7093	1.2837	−0.540 26	−0.113 95
0.2	−1.2609	−0.706 15	2.4091	0.986 64	2.7091	1.2828	−0.541 83	−0.115 28
0.3	−1.2618	−0.704 53	2.4080	0.982 84	2.7080	1.2769	−0.552 56	−0.124 36
0.4	−1.2638	−0.697 89	2.4048	0.968 87	2.7046	1.2555	−0.593 03	−0.158 79
0.5	−1.2612	−0.674 99	2.3994	0.931 86	2.7021	1.2004	−0.707 71	−0.257 74
0.6	−1.2115	−0.596 01	2.4011	0.851 54	2.7304	1.0891	−0.992 01	−0.509 25
0.7	−0.903 65	−0.299 57	2.4498	0.693 75	2.9141	0.8996	−1.6680	−1.1160
0.8	0.749 10	1.0075	2.6648	0.361 71	3.6445	0.5639	−3.3135	−2.4986
0.9	13.491	10.277	3.4655	−0.674 81	6.3098	−0.4646	−8.3283	−6.1156
$\theta_0 = 60^\circ$								
0.0	−3.7205	−1.4932	3.6640	1.6104	3.8492	2.0245	−0.573 67	0.217 02
0.1	−3.7210	−1.4932	3.6639	1.6101	3.8490	2.0241	−0.574 40	0.216 38
0.2	−3.7290	−1.4926	3.6627	1.6062	3.8462	2.0181	−0.584 89	0.207 16
0.3	−3.7611	−1.4892	3.6584	1.5900	3.8355	1.9934	−0.629 80	0.167 19
0.4	−3.8354	−1.4735	3.6503	1.5478	3.8149	1.9305	−0.754 61	0.052 73
0.5	−3.9396	−1.4080	3.6466	1.4619	3.8058	1.8096	−1.0439	−0.226 27
0.6	−3.9260	−1.1545	3.6803	1.3091	3.9032	1.6188	−1.6713	−0.864 77
0.7	−3.1285	−0.193 36	3.8422	1.0442	4.3899	1.3477	−3.0166	−2.2332
0.8	1.7161	3.8947	4.3398	0.502 09	5.9802	0.860 45	−6.0081	−4.8447
0.9	39.837	32.072	5.8808	−1.2416	11.085	−0.847 27	−14.725	−11.053

finding a time-periodic solution of (30)–(36) implying the steady-state wave regimes. The lowest-order generalized coordinates $r_1(t)$ and $p_1(t)$ are presented by the Fourier series

$$r_1(t) = \sum_{k=1}^{\infty}(A_{2k-1}\cos(k\sigma t) + A_{2k}\sin(k\sigma t)), \qquad p_1(t) = \sum_{k=1}^{\infty}(B_{2k-1}\cos(k\sigma t) + B_{2k}\sin(k\sigma t)),$$

where, according to the Moiseev asymptotics, the leading asymptotic contribution is associated with the first harmonics, i.e.

$$r_1(t) = A_1\cos\sigma t + A_2\sin\sigma t + o(\epsilon^{1/3}); \qquad p_1(t) = B_1\cos\sigma t + B_2\sin\sigma t + o(\epsilon^{1/3}) \tag{38}$$

and $A_1 \sim A_2 \sim B_1 \sim B_2 = O(\epsilon^{1/3})$, $\epsilon = H$.

As follows from substituting (38) into the modal equations (30), (33) and (34), the generalized coordinates $p_0(t)$, $r_2(t)$ and $p_2(t)$ are functions of the dominant amplitude

Table 2. Non-dimensional hydrodynamic coefficients $\mathtt{d_i}$ ($i = 9, \ldots, 15$) computed within the five significant figures.

$\mathtt{r_1}$	$\mathtt{d_9}$	$\mathtt{d_{10}}$	$\mathtt{d_{11}}$	$\mathtt{d_{12}}$	$\mathtt{d_{13}}$	$\mathtt{d_{14}}$	$\bar{\mathtt{d}}_{15}$
$\theta_0 = 30^\circ$							
0.0	1.4942	0.947 38	0.592 58	0.046 99	2.0917	1.2362	−2.0910
0.1	1.4942	0.947 38	0.592 58	0.046 99	2.0917	1.2362	−2.0910
0.2	1.4942	0.947 38	0.592 59	0.047 04	2.0917	1.2362	−2.0910
0.3	1.4942	0.947 31	0.592 80	0.048 05	2.0917	1.2361	−2.0919
0.4	1.4939	0.946 75	0.594 35	0.055 62	2.0916	1.2361	−2.0988
0.5	1.4918	0.944 03	0.601 86	0.092 39	2.0910	1.2357	−2.1317
0.6	1.4777	0.932 62	0.631 31	0.237 91	2.0873	1.2314	−2.2562
0.7	1.3954	0.882 93	0.745 53	0.814 12	2.0567	1.1960	−2.6836
0.8	0.976 47	0.656 23	1.3319	3.6853	1.7952	0.938 05	−4.1936
0.9	−1.0481	−0.342 31	7.6923	29.046	−0.285 13	−0.827 51	−10.602
$\theta_0 = 45^\circ$							
0.0	2.4532	2.0600	1.5573	−0.106 32	3.3797	2.0406	−2.2336
0.1	2.4533	2.0600	1.5573	−0.106 25	3.3797	2.0406	−2.2336
0.2	2.4536	2.0600	1.5578	−0.103 91	3.3801	2.0406	−2.2357
0.3	2.4554	2.0603	1.5615	−0.087 57	3.3828	2.0407	−2.2500
0.4	2.4603	2.0604	1.5760	−0.022 59	3.3927	2.0409	−2.3061
0.5	2.4621	2.0542	1.6192	0.185 36	3.4174	2.0385	−2.4758
0.6	2.4205	2.0087	1.7407	0.839 90	3.4553	2.0139	−2.9347
0.7	2.1786	1.8011	2.1378	3.1767	3.4196	1.8650	−4.1575
0.8	1.2347	1.1195	4.1352	13.820	2.7763	1.1277	−7.6159
0.9	−2.3343	−0.785 01	24.725	95.558	−1.2179	−2.2344	−19.347
$\theta_0 = 60^\circ$							
0.0	4.1682	4.3989	4.4451	−0.291 65	5.7152	3.4673	−2.7985
0.1	4.1685	4.3990	4.4455	−0.290 35	5.7155	3.4674	−2.7994
0.2	4.1722	4.4008	4.4507	−0.271 58	5.7202	3.4677	−2.8131
0.3	4.1858	4.4069	4.4733	−0.187 49	5.7400	3.4690	−2.8739
0.4	4.2106	4.4138	4.5367	0.07251	5.7924	3.4710	−3.0538
0.5	4.2226	4.3879	4.6888	0.81501	5.8945	3.4638	−3.5037
0.6	4.1197	4.2067	5.0618	3.0797	6.0249	3.3930	−4.5695
0.7	3.5918	3.5520	6.2379	11.025	5.9604	3.0276	−7.1431
0.8	1.8087	1.9574	12.419	45.741	4.6430	1.5193	−13.761
0.9	−4.3714	−1.4656	75.970	298.86	−2.5376	−4.3806	−34.457

parameters A_1, A_2, B_1 and B_2, i.e.

$$p_0(t) = -\left(A_1^2 + A_2^2 + B_1^2 + B_2^2\right) o_0^{(0)} - \tfrac{1}{2}\left(A_1^2 - A_2^2 + B_1^2 - B_2^2\right) o_0^{(2)} \cos 2\sigma t - \left(A_1 A_2 + B_1 B_2\right) o_0^{(2)} \sin 2\sigma t + o\left(\epsilon^{2/3}\right), \tag{39}$$

$$r_2(t) = -2\left(A_1 B_1 + A_2 B_2\right) o_2^{(0)} - \left(A_1 B_1 - A_2 B_2\right) o_2^{(2)} \cos 2\sigma t - \left(A_1 B_2 + A_2 B_1\right) o_2^{(2)} \sin 2\sigma t + o(\epsilon^{2/3}), \tag{40}$$

$$p_2(t) = \left(A_1^2 + A_2^2 - B_1^2 - B_2^2\right) o_2^{(0)} + \tfrac{1}{2}\left(A_1^2 - A_2^2 - B_1^2 + B_2^2\right) o_2^{(2)} \cos 2\sigma t + \left(A_1 A_2 - B_1 B_2\right) o_2^{(2)} \sin 2\sigma t + o(\epsilon^{2/3}). \tag{41}$$

Table 3. Non-dimensional hydrodynamic coefficients $\mathtt{g_j}$ $(j = 0, 1, \ldots, 6)$ computed within the five significant figures.

$\mathtt{r_1}$	$\mathtt{g_0}$	$\mathtt{g_1}$	$\mathtt{g_2}$	$\mathtt{g_3}$	$\mathtt{g_4}$	$\mathtt{g_5}$	$\mathtt{g_6}$
$\theta_0 = 30^\circ$							
0.0	0.210 45	0.936 12	0.828 77	−0.373 19	0.561 56	1.1259	0.079 39
0.1	0.210 45	0.936 12	0.828 77	−0.373 19	0.561 56	1.1259	0.079 39
0.2	0.210 45	0.936 11	0.828 77	−0.373 19	0.561 57	1.1259	0.079 39
0.3	0.210 45	0.935 98	0.828 75	−0.373 24	0.561 61	1.1259	0.079 40
0.4	0.210 40	0.934 99	0.828 56	−0.373 65	0.561 95	1.1262	0.079 46
0.5	0.210 19	0.930 55	0.827 77	−0.375 49	0.563 44	1.1276	0.079 72
0.6	0.209 38	0.916 53	0.825 81	−0.381 64	0.568 03	1.1326	0.080 58
0.7	0.206 46	0.886 30	0.824 31	−0.397 56	0.578 12	1.1474	0.082 80
0.8	0.197 05	0.856 42	0.835 81	−0.429 05	0.591 16	1.1782	0.086 64
0.9	0.177 78	0.892 85	0.885 71	−0.471 53	0.592 66	1.1977	0.088 40
$\theta_0 = 45^\circ$							
0.0	0.424 46	1.5482	1.3767	−1.0000	0.967 84	1.9415	0.236 40
0.1	0.424 46	1.5482	1.3767	−1.0000	0.967 85	1.9415	0.236 40
0.2	0.424 42	1.5476	1.3766	−1.0004	0.968 02	1.9416	0.236 45
0.3	0.424 17	1.5439	1.3758	−1.0028	0.969 16	1.9426	0.236 77
0.4	0.423 17	1.5308	1.3732	−1.0118	0.973 16	1.9463	0.237 95
0.5	0.420 04	1.4987	1.3680	−1.0356	0.982 85	1.9571	0.241 07
0.6	0.411 29	1.4431	1.3631	−1.0859	1.0005	1.9826	0.247 59
0.7	0.389 72	1.3877	1.3727	−1.1740	1.0233	2.0302	0.258 21
0.8	0.348 53	1.4089	1.4275	−1.2982	1.0374	2.0863	0.268 77
0.9	0.302 14	1.5593	1.5441	−1.4306	1.0269	2.0818	0.266 32
$\theta_0 = 60^\circ$							
0.0	0.847 32	2.5394	2.3194	−2.7525	1.6750	3.3611	0.708 93
0.1	0.847 28	2.5390	2.3193	−2.7529	1.6751	3.3612	0.708 98
0.2	0.846 78	2.5340	2.3181	−2.7585	1.6766	3.3623	0.709 65
0.3	0.844 57	2.5133	2.3134	−2.7820	1.6824	3.3674	0.712 50
0.4	0.837 93	2.4628	2.3031	−2.8438	1.6966	3.3822	0.720 02
0.5	0.821 20	2.3737	2.2894	−2.9712	1.7225	3.4160	0.735 48
0.6	0.783 79	2.2649	2.2857	−3.1932	1.7596	3.4801	0.761 71
0.7	0.711 13	2.2159	2.3265	−3.5243	1.7967	3.5768	0.796 60
0.8	0.603 75	2.3582	2.4590	−3.9380	1.8086	3.6610	0.821 65
0.9	0.508 62	2.6915	2.6835	−4.3466	1.7800	3.6193	0.802 77

Analogously, one can find

$$r_3(t) = (A_1(A_1^2 + A_2^2 - 3B_1^2 - B_2^2) - 2A_2B_1B_2)o_3^{(1)} \cos\sigma t + (A_2(A_1^2 + A_2^2 - B_1^2 - 3B_2^2) - 2A_1B_1B_2)o_3^{(1)} \sin\sigma t + (A_1(A_1^2 - 3A_2^2 - 3B_1^2 + 3B_2^2) + 6A_2B_1B_2)o_3^{(3)} \cos 3\sigma t + (A_2(3A_1^2 - A_2^2 - 3B_1^2 + 3B_2^2) - 6A_1B_1B_2)o_3^{(3)} \sin 3\sigma t + o(\epsilon), \quad (42)$$

$$p_3(t) = (B_1(3A_1^2 + A_2^2 - B_1^2 - B_2^2) + 2A_1A_2B_2)o_3^{(1)} \cos\sigma t + (B_2(A_1^2 + 3A_2^2 - B_1^2 - B_2^2) + 2A_1A_2B_1)o_3^{(1)} \sin\sigma t + (B_1(3A_1^2 - 3A_2^2 - B_1^2 + 3B_2^2) - 6A_1A_2B_2)o_3^{(3)} \cos 3\sigma t + (B_2(3A_1^2 - 3A_2^2 - 3B_1^2 + B_2^2) + 6A_1A_2B_1)o_3^{(3)} \sin 3\sigma t + o(\epsilon), \quad (43)$$

where coefficients o_m^k are defined in appendix A.

Substituting (38), (39)–(41) into the modal equations (32) and (31) and gathering the lowest-order terms at the first harmonics lead to the system of algebraic equations

$$\begin{cases} (m_1(A_1^2+A_2^2+B_1^2)+m_2B_2^2)A_1+m_3A_2B_1B_2+(\bar\sigma_1^2-1)A_1=H\Lambda, \\ (m_1(A_1^2+A_2^2+B_2^2)+m_2B_1^2)A_2+m_3A_1B_1B_2+(\bar\sigma_1^2-1)A_2=0, \\ (m_1(A_1^2+B_1^2+B_2^2)+m_2A_2^2)B_1+m_3A_1A_2B_2+(\bar\sigma_1^2-1)B_1=0, \\ (m_1(A_2^2+B_1^2+B_2^2)+m_2A_1^2)B_2+m_3A_1A_2B_1+(\bar\sigma_1^2-1)B_2=0 \end{cases} \tag{44}$$

with respect to the dominant amplitude parameters, where coefficients m_i depend on hydrodynamic coefficients of the modal equations; see formulae (B.1) in appendix A.

The algebraic system (44) is similar to those by Gavrilyuk *et al* (2005) where we showed that its solvability condition consists of $A_2=B_1=0$ and, therefore, there are only two non-zero amplitude parameters which can be found from the system

$$m_1A_1^3+m_2A_1B_2^2+\left(\bar\sigma_1^2-1\right)A_1=H\Lambda, \quad m_1B_2^3+m_2A_1^2B_2+\left(\bar\sigma_1^2-1\right)B_2=0, \tag{45}$$

whose solution obviously depends on m_i and, in turn, on the non-dimensional ratio of the bottom and free surface radii $\mathfrak{r}_1$, $\bar\sigma_1(\mathfrak{r}_1)$ and θ_0 ($m_i=m_i(\bar\sigma_1,\mathfrak{r}_1,\theta_0)$).

As shown by Gavrilyuk *et al* (2005), one can distinguish two types of solutions of (45) and the corresponding steady-state wave regimes. The first solution type, $A_1\neq0$, $B_2=0$, implies the so-called planar waves. The second solution type, $A_1\neq0$, $B_2\neq0$, leads to the so-called swirling. The planar waves are described by the asymptotic solution

$$\begin{aligned} &p_1=r_2=p_3=0, \quad r_1=A_1\cos\sigma t+o(\epsilon), \quad p_2=A_1^2o_2^{(0)}+\tfrac12A_1^2o_2^{(2)}\cos2\sigma t+o(\epsilon^2), \\ &r_3=A_1^3o_3^{(1)}\cos\sigma t+A_1^3o_3^{(3)}\cos3\sigma t+o(\epsilon^3), \quad p_0=-A_1^2o_0^{(0)}-\tfrac12A_1^2o_0^{(2)}\cos2\sigma t+o(\epsilon^2), \end{aligned} \tag{46}$$

where the amplitude parameter A_1 is the root of the cubic equation

$$m_1\,A_1^3+(\bar\sigma_1^2-1)\,A_1-H\Lambda=0. \tag{47}$$

Swirling implies

$$\begin{aligned} &r_1(t)=A_1\cos\sigma t+o(\epsilon), \quad p_1(t)=B_2\sin\sigma t+o(\epsilon), \\ &r_2(t)=-A_1B_2o_2^{(2)}\sin2\sigma t+o(\epsilon^2), \\ &p_0(t)=-\left(A_1^2+B_2^2\right)o_0^{(0)}-\tfrac12\left(A_1^2-B_2^2\right)o_0^{(2)}\cos2\sigma t+o(\epsilon^2), \\ &p_2(t)=\left(A_1^2-B_2^2\right)o_2^{(0)}+\tfrac12\left(A_1^2+B_2^2\right)o_2^{(2)}\cos2\sigma t+o(\epsilon^2), \\ &r_3(t)=A_1(A_1^2-B_2^2)o_3^{(1)}\cos\sigma t+A_1(A_1^2+3B_2^2)o_3^{(3)}\cos3\sigma t+o(\epsilon^3), \\ &p_3(t)=B_2(A_1^2-B_2^2)o_3^{(1)}\sin\sigma t+B_2(3A_1^2+B_2^2)o_3^{(3)}\sin3\sigma t+o(\epsilon^3), \end{aligned} \tag{48}$$

where the amplitude parameters A_1 and B_2 are computed from the equations

$$m_6A_1^3+m_5(\bar\sigma_1^2-1)A_1-H\Lambda=0, \quad B_2^2=(m_1A_1^2-(\bar\sigma_1^2-1))/m_2>0, \tag{49}$$

$m_5=m_3/m_1$ and $m_6=m_4m_5$. The latter inequality in (49) is the solvability condition.

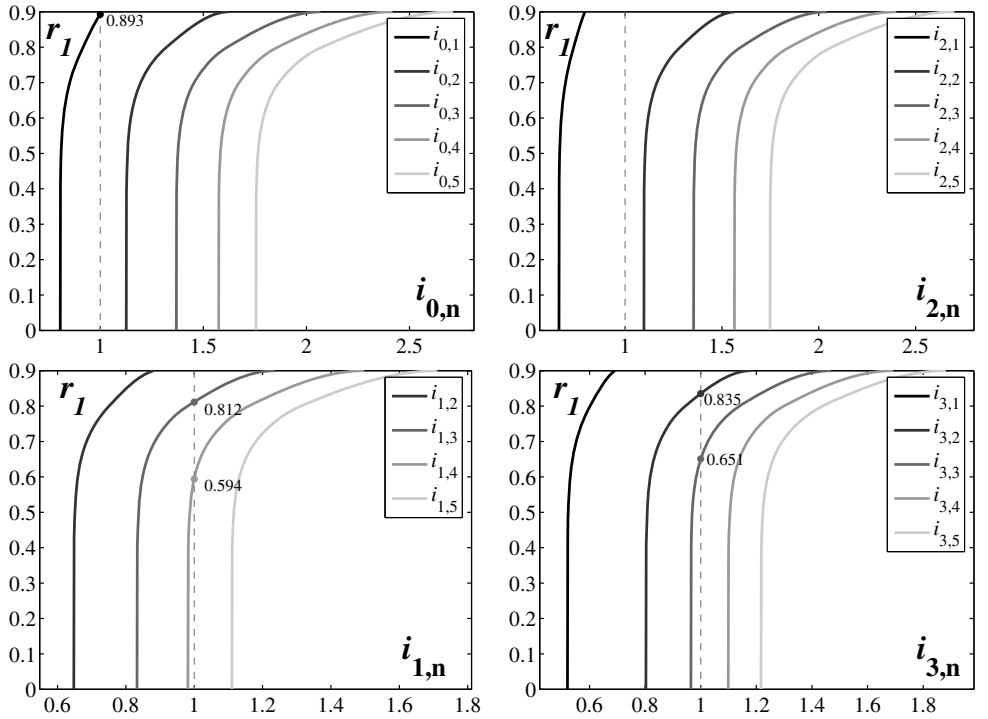

Figure 6. The graphs of $\mathtt{r}_1 = \mathtt{r}_1(i_{m,n})$ ($\mathtt{r}_1$ is the ratio of the bottom and free surface radii) for the semi-apex angle $\theta_0 = 30^\circ$. The secondary resonance is expected at $\mathtt{r}_1 = 0.8116$, 0.5939, 0.8926, 0.835 and 0.651.

6. Secondary resonances

When constructing the time-periodic solution, we assumed that the forcing frequency σ is close to the lowest natural sloshing frequency σ_{11}, i.e.

$$\sigma \approx \sigma_{11}. \tag{50}$$

The constructed solution is valid if and only if coefficients in front of the polynomial terms by the amplitude parameters are of the order $O(1)$. However, these coefficients become large when 2σ is close to one from the natural sloshing frequencies σ_{2i} and σ_{0i}, $i \geqslant 1$, or, alternatively, when 3σ tends to one from the natural sloshing frequencies σ_{3i}, $i \geqslant 1$ and σ_{1i}, $i \geqslant 2$. This closeness is associated with the so-called *secondary resonances*. The necessary condition of the secondary resonance consists of satisfying the relations

$$2\sigma \approx \sigma_{0n}, \quad 2\sigma \approx \sigma_{2n}, \quad 3\sigma \approx \sigma_{3n}, \quad 3\sigma \approx \sigma_{1(n+1)}, \quad n \geqslant 1 \tag{51}$$

together with (50). The secondary resonance is not avoidable with the strong equalities in (51) and (50).

To analyze the secondary resonances with strong equalities in (51) and (50), we plot in figures 6–8 the graphs of $i_{m,n}(\theta_0, \mathtt{r}_1)$ as functions of the non-dimensional parameter $\mathtt{r}_1$ ($\mathtt{r}_1$ is

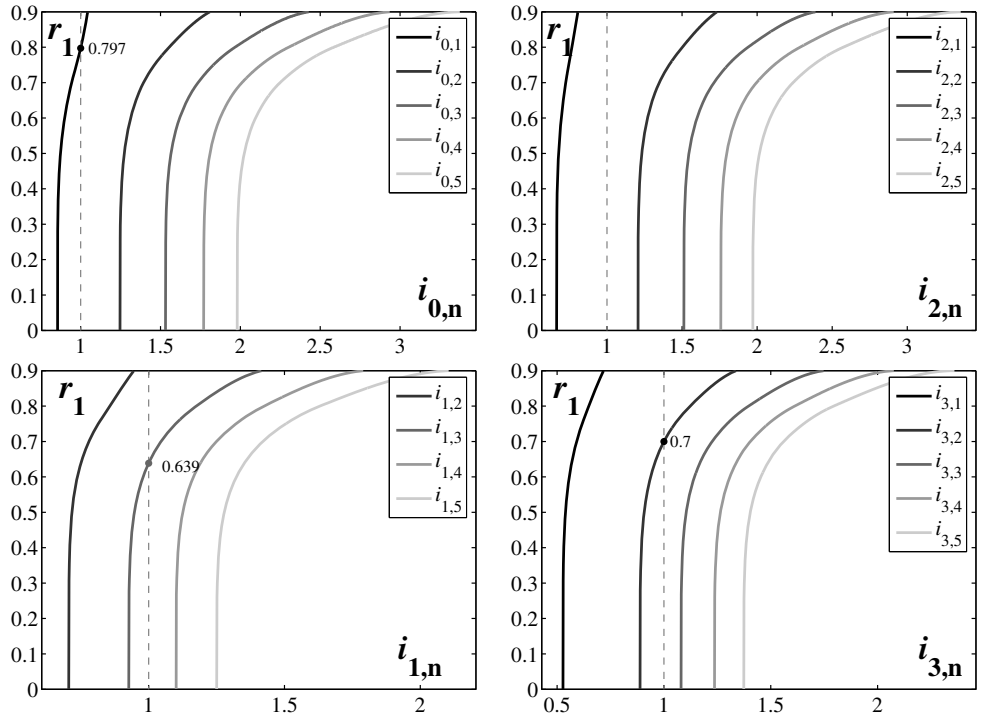

Figure 7. The graphs of $\mathtt{r}_1 = \mathtt{r}_1(i_{m,n})$ ($\mathtt{r}_1$ is the ratio of the bottom and free surface radii) for the semi-apex angle $\theta_0 = 45^\circ$. The secondary resonance is expected at $\mathtt{r}_1 = 0.6386$, 0.7972 and 0.7.

the ratio of the bottom and free surface radii) with a fixed value of the semi-apex angle

$$i_{0,n}(\theta_0, \mathtt{r}_1) = \frac{\sigma_{0n}}{2\sigma_{11}} = \frac{1}{2}\sqrt{\frac{\kappa_{0n}}{\kappa_{11}}}, \quad i_{2,n}(\theta_0, \mathtt{r}_1) = \frac{\sigma_{2n}}{2\sigma_{11}} = \frac{1}{2}\sqrt{\frac{\kappa_{2n}}{\kappa_{11}}},$$
$$i_{3,n}(\theta_0, \mathtt{r}_1) = \frac{\sigma_{3n}}{3\sigma_{11}} = \frac{1}{3}\sqrt{\frac{\kappa_{3n}}{\kappa_{11}}}, \quad i_{1(n+1)}(\theta_0, \mathtt{r}_1) = \frac{\sigma_{1(n+1)}}{3\sigma_{11}} = \frac{1}{3}\sqrt{\frac{\kappa_{1(n+1)}}{\kappa_{11}}}, \quad n \geqslant 1. \tag{52}$$

The functions $i_{m,n} = i_{m,n}(\theta_0, \mathtt{r}_1)$ do not depend on the forcing frequency σ and one can see that the condition

$$i_{m,n} = 1 \tag{53}$$

for certain indices m and n is equivalent to the strong equality in the corresponding m, n-equation of (51) and (50), simultaneously. The case $\mathtt{r}_1 = 0$ corresponds to the V-shaped conical tank but the limit $\mathtt{r}_1 \to 1$ implies the shallow water condition.

The calculations were done for the three semi-apex angles $\theta_0 = 30^\circ$, 45° and 60°. The strong equality $i_{0,1} = 1$ happens for $\mathtt{r}_1 = 0.8926$ implying that the first axisymmetric mode is subject of the secondary resonance for larger $\mathtt{r}_1$ and the double harmonics 2σ can then be amplified. As for the triple harmonics 3σ, it can occur for the modes (1,3), (1,4), (3,2) and (3,3). So, for $\mathtt{r}_1 = 0.651$, the modes (3,3) are subject to the secondary resonance but the modes (3,2) is resonantly excited at $\mathtt{r}_1 = 0.835$. Finally, the modes (1,3) are exposed to the secondary resonance at $\mathtt{r}_1 = 0.8116$ and the modes (1,4) at $\mathtt{r}_1 = 0.5939$. The strong secondary

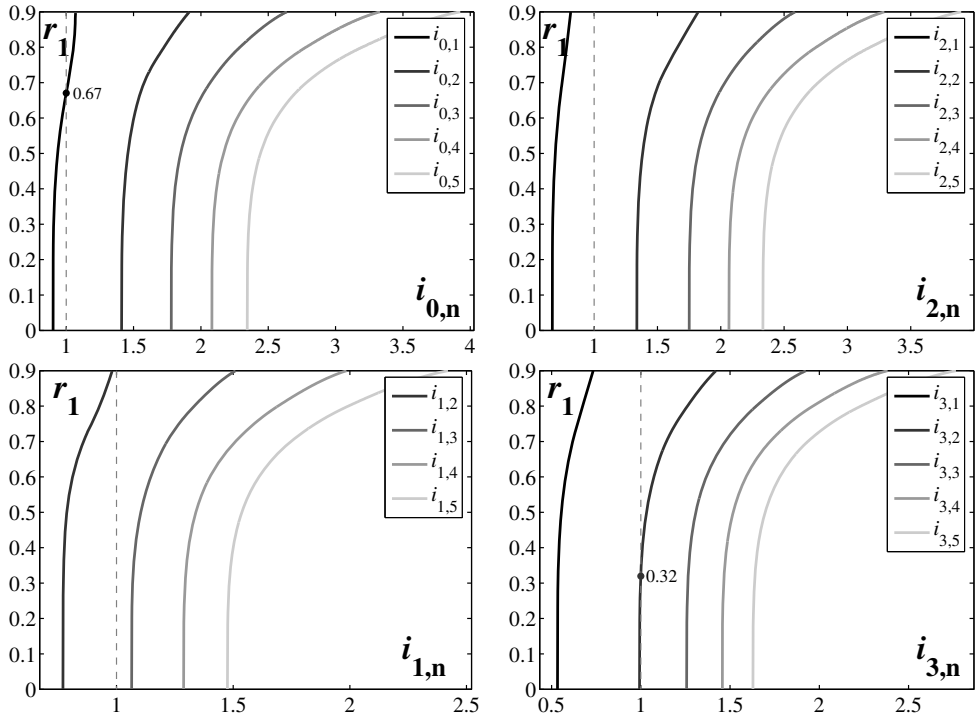

Figure 8. The graphs of $\mathtt{r}_1 = \mathtt{r}_1(i_{m,n})$ ($\mathtt{r}_1$ is the ratio of of the bottom and free surface radii) for the semi-apex angle $\theta_0 = 60^\circ$. The secondary resonance is expected as $\mathtt{r}_1 = 0.67$ and 0.3196.

resonances for the semi-apex angle $\theta_0 = 30^\circ$ are not expected for the non-dimensional ratio $\mathtt{r}_1 \lesssim 0.5$.

As follows from figure 7, the secondary resonances also exist for $\theta_0 = 45^\circ$ at $\mathtt{r}_1 = 0.6386$ (modes (1,3)), $\mathtt{r}_1 = 0.7972$ (mode (0,1)) and $\mathtt{r}_1 = 0.7$ (modes (3,2)). This implies that the constructed Moiseev type modal equations can be applicable for the non-dimensional ratios $\mathtt{r}_1 \lesssim 0.6$. Figure 8 demonstrates two critical values of $\mathtt{r}_1$ for $\theta_0 = 60^\circ$. These are $\mathtt{r}_1 = 0.67$ (the secondary resonance by the mode (0,1)) and $\mathtt{r}_1 = 0.3196$ (the secondary resonance for the modes (3,2)). Moreover, $i_{3,2}$ is close to 1 for $\mathtt{r}_1 \lesssim 0.5$ but $i_{0,1} \approx 1$ for $0.55 \lesssim \mathtt{r}_1$. This means that the derived modal equations may need revision accounting for secondary resonances for this semi-apex angle.

7. Stability analysis

The hydrodynamic instability of the time-periodic solutions (46) and (48) can be studied by employing the first Lyapunov method. This implies introducing small perturbations of these solutions denoted by α, β, η, γ, δ, μ and ν, i.e. $p_0(t) = \tilde{p}_0(t) + \eta(t)$, $p_1(t) = \tilde{p}_1(t) + \beta(t)$, $r_1(t) = \tilde{r}_1(t) + \alpha(t)$, $p_2(t) = \tilde{p}_2(t) + \delta(t)$, $r_2(t) = \tilde{r}_2(t) + \gamma(t)$, $p_3(t) = \tilde{p}_3(t) + \nu(t)$, $r_3(t) = \tilde{r}_3(t) + \mu(t)$, and constructing the following linear differential variational equations with respect to α, β, η, γ, δ, μ, ν:

$$\ddot{\eta} + \sigma_0^2\eta + \mathtt{d}_{10}(\ddot{r}_1\alpha + \ddot{p}_1\beta + \ddot{\alpha}r_1 + \ddot{\beta}p_1) + 2\mathtt{d}_8(\dot{\alpha}\dot{r}_1 + \dot{\beta}\dot{p}_1) + 2\sigma_0^2\mathtt{g}_0(\alpha r_1 + \beta p_1) = 0,$$

$$\begin{aligned}
&\ddot{\alpha}+\sigma_1^2\alpha+\mathtt{d}_1(\alpha(\dot{p}_1^2+\dot{r}_1^2+\ddot{p}_1p_1+2\ddot{r}_1r_1)+r_1(\dddot{\beta}p_1+\ddot{\alpha}r_1+\ddot{p}_1\beta+2\dot{\beta}\dot{p}_1+2\dot{\alpha}\dot{r}_1))\\
&\qquad+\mathtt{d}_2(p_1(\ddot{\alpha}p_1-\dddot{\beta}r_1+2\dot{\alpha}\dot{p}_1)+\beta(2\dot{p}_1\dot{r}_1+2p_1\ddot{r}_1-r_1\ddot{p}_1)-\alpha(\ddot{p}_1p_1+2\dot{p}_1^2)\\
&\qquad+2\dot{\beta}(\dot{r}_1p_1-2\dot{p}_1r_1))+\mathtt{d}_3(\dddot{\beta}r_2-\ddot{\alpha}p_2+\dot{\beta}\dot{r}_2-\dot{\alpha}\dot{p}_2+\dot{\gamma}\dot{p}_1-\dot{\delta}\dot{r}_1+\gamma\ddot{p}_1-\delta\ddot{r}_1)\\
&\qquad+\mathtt{d}_4(\beta\ddot{r}_2-\alpha\ddot{p}_2+\ddot{\gamma}p_1-\ddot{\delta}r_1)+\mathtt{d}_5(\ddot{\alpha}p_0+\dot{\alpha}\dot{p}_0+\dot{\eta}\dot{r}_1+\eta\ddot{r}_1)+\mathtt{d}_6(\alpha\ddot{p}_0+\ddot{\eta}r_1)\\
&\qquad+\sigma_1^2(\mathtt{g}_1(\alpha p_0+\eta r_1)+\mathtt{g}_2(\beta r_2-\alpha p_2+\gamma p_1-\delta r_1)\\
&\qquad+\mathtt{g}_3(2\beta p_1r_1+\alpha(p_1^2+3r_1^2)))=0,
\end{aligned}$$

$$\begin{aligned}
&\ddot{\beta}+\sigma_1^2\beta+\mathtt{d}_1(\beta(\dot{p}_1^2+\dot{r}_1^2+2\ddot{p}_1p_1+\ddot{r}_1r_1)+p_1(\dddot{\beta}p_1+2\dot{\beta}\dot{p}_1+\ddot{\alpha}r_1+2\dot{\alpha}\dot{r}_1+\alpha\ddot{r}_1))\\
&\qquad+\mathtt{d}_2(r_1(\dddot{\beta}r_1+2\dot{\beta}\dot{r}_1-\ddot{\alpha}p_1)+\alpha(2\ddot{p}_1r_1+2\dot{p}_1\dot{r}_1-\ddot{r}_1p_1)-\beta(\ddot{r}_1r_1+2\dot{r}_1^2)\\
&\qquad+2\dot{\alpha}(\dot{p}_1r_1-2\dot{r}_1p_1))+\mathtt{d}_3(\dddot{\beta}p_2+\ddot{\beta}\dot{p}_2+\ddot{\alpha}r_2+\dot{\alpha}\dot{r}_2+\dot{\delta}\dot{p}_1+\delta\ddot{p}_1+\dot{\gamma}\dot{r}_1+\gamma\ddot{r}_1)\\
&\qquad+\mathtt{d}_4(\ddot{\delta}p_1+\ddot{\gamma}r_1+\alpha\ddot{r}_2+\beta\ddot{p}_2)+\mathtt{d}_5(\ddot{\beta}p_0+\dot{\beta}\dot{p}_0+\dot{\eta}\dot{p}_1+\eta\ddot{p}_1)+\mathtt{d}_6(\beta\ddot{p}_0+\ddot{\eta}p_1)\\
&\qquad+\sigma_1^2(\mathtt{g}_1(\beta p_0+\eta p_1)+\mathtt{g}_2(\alpha r_2+\beta p_2+\gamma r_1+\delta p_1)\\
&\qquad+\mathtt{g}_3(2\alpha p_1r_1+\beta(3p_1^2+r_1^2)))=0,
\end{aligned}$$

$$\ddot{\gamma}+\sigma_2^2\gamma+\mathtt{d}_9(\ddot{p}_1\alpha+\ddot{r}_1\beta+\ddot{\alpha}p_1+\ddot{\beta}r_1)+2\mathtt{d}_7(\dot{\alpha}\dot{p}_1+\dot{\beta}\dot{r}_1)+2\sigma_2^2\mathtt{g}_4(\alpha p_1+\beta r_1)=0,$$

$$\ddot{\delta}+\sigma_2^2\delta+\mathtt{d}_9(\ddot{r}_1\alpha-\ddot{\beta}p_1-\ddot{\alpha}r_1-\ddot{p}_1\beta)+2\mathtt{d}_7(\dot{\beta}\dot{p}_1-\dot{\alpha}\dot{r}_1)+2\sigma_2^2\mathtt{g}_4(\beta p_1-\alpha r_1)=0,$$

$$\begin{aligned}
&\ddot{\mu}+\sigma_3^2\mu+\mathtt{d}_{11}(\ddot{\alpha}(p_1^2-r_1^2)+2\ddot{\beta}p_1r_1+2\alpha(\ddot{p}_1p_1-\ddot{r}_1r_1)+2\beta(\ddot{p}_1r_1+\ddot{r}_1p_1))\\
&\qquad+\mathtt{d}_{12}(2\dot{\alpha}(p_1\dot{p}_1-r_1\dot{r}_1)+\alpha(\dot{p}_1^2-\dot{r}_1^2)+2\dot{\beta}(p_1\dot{r}_1+r_1\dot{p}_1)+2\beta\dot{p}_1\dot{r}_1)\\
&\qquad+\mathtt{d}_{13}(\ddot{\alpha}p_2+\ddot{\beta}r_2+\delta\ddot{r}_1+\gamma\ddot{p}_1)+\mathtt{d}_{14}(\alpha\ddot{p}_2+\beta\ddot{r}_2+\ddot{\gamma}p_1+\ddot{\delta}r_1)\\
&\qquad+\mathtt{d}_{15}(\dot{\alpha}\dot{p}_2+\dot{\beta}\dot{r}_2+\dot{\gamma}\dot{p}_1+\dot{\delta}\dot{r}_1)+\sigma_3^2(\mathtt{g}_5(\alpha p_2+\beta r_2+\delta r_1+\gamma p_1)\\
&\qquad+3\mathtt{g}_6(\alpha(p_1^2-r_1^2)+2\beta p_1r_1))=0,
\end{aligned}$$

$$\begin{aligned}
&\ddot{\nu}+\sigma_3^2\nu+\mathtt{d}_{11}(\ddot{\beta}(p_1^2-r_1^2)-2\ddot{\alpha}p_1r_1+2\beta(p_1\ddot{p}_1-r_1\ddot{r}_1)-2\alpha(r_1\ddot{p}_1+p_1\ddot{r}_1))\\
&\qquad+\mathtt{d}_{12}(2\dot{\beta}(p_1\dot{p}_1-r_1\dot{r}_1)-2\dot{\alpha}(r_1\dot{p}_1+p_1\dot{r}_1)+\beta(\dot{p}_1^2-\dot{r}_1^2)-2\alpha\dot{p}_1\dot{r}_1)\\
&\qquad+\mathtt{d}_{13}(\ddot{\beta}p_2-\ddot{\alpha}r_2+\delta\ddot{p}_1-\gamma\ddot{r}_1)+\mathtt{d}_{14}(\beta\ddot{p}_2-\alpha\ddot{r}_2+\ddot{\delta}p_1-\ddot{\gamma}r_1)\\
&\qquad+\mathtt{d}_{15}(\dot{\beta}\dot{p}_2-\dot{\alpha}\dot{r}_2+\dot{\delta}\dot{p}_1-\dot{\gamma}\dot{r}_1)+\sigma_3^2(\mathtt{g}_5(\beta p_2-\alpha r_2+\delta p_1-\gamma r_1)\\
&\qquad+3\mathtt{g}_6(\beta(p_1^2-r_1^2)-2\alpha p_1r_1))=0.
\end{aligned}$$

Here, $\mathtt{d}_i$ ($i=1,\ldots,15$) and $\mathtt{g}_j$ ($j=0,\ldots,6$) are the coefficients of derived nonlinear modal system.

Equations above constitute a system of linear ordinary differential equations with periodic coefficients. Its fundamental solution can be obtained by employing the Floquet theory suggesting the solution

$$\begin{aligned}
&\alpha(t)=\mathrm{e}^{\lambda t}\psi_1(t),\quad \beta(t)=\mathrm{e}^{\lambda t}\psi_2(t),\quad \gamma(t)=\mathrm{e}^{\lambda t}\psi_3(t),\quad \delta(t)=\mathrm{e}^{\lambda t}\psi_4(t),\\
&\eta(t)=\mathrm{e}^{\lambda t}\psi_5(t),\quad \mu(t)=\mathrm{e}^{\lambda t}\psi_6(t),\quad \nu(t)=\mathrm{e}^{\lambda t}\psi_7(t),
\end{aligned}\tag{54}$$

where λ is the characteristic exponent and ψ_i are the $2\pi/\sigma$–periodic functions. The instability of (46) and (48), as follows from the expressions (54), depends on the values λ. At least one of the values should have the positive real part.

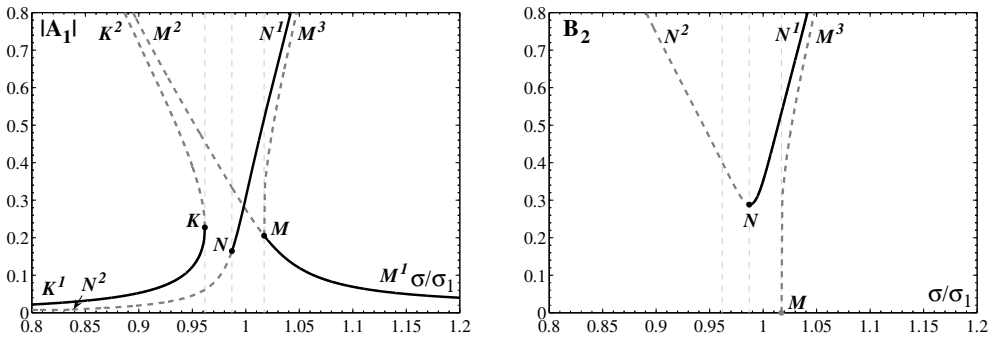

Figure 9. The response curves for planar and swirling resonant steady-state sloshing drawn for the semi-apex angle $\theta_0 = 30^\circ$, the non-dimensional ratio $\mathtt{r}_1 = 0.5$ and the non-dimensional excitation amplitude $H = 0.01$. The amplitude parameters A_1 and B_2 imply longitudinal and transverse wave components.

To get the characteristic exponent approximate values we pose the periodic functions $\psi_1(t)$ and $\psi_2(t)$ in the Fourier series

$$\psi_1(t) = a_1 \cos\sigma t + a_2 \sin\sigma t + \cdots, \qquad \psi_2(t) = b_1 \cos\sigma t + b_2 \sin\sigma t + \cdots \tag{55}$$

and substitute them, together with (54), into equations in variations. Using the Bubnov–Galerkin method leads to the following system of linear homogeneous equations:

$$\begin{aligned} &\mathbb{C}_{11}a_1 + \mathbb{C}_{12}a_2 + \mathbb{C}_{13}b_1 + \mathbb{C}_{14}b_2 = 0,\\ &\mathbb{C}_{21}a_1 + \mathbb{C}_{22}a_2 + \mathbb{C}_{23}b_1 + \mathbb{C}_{24}b_2 = 0,\\ &\mathbb{C}_{31}a_1 + \mathbb{C}_{32}a_2 + \mathbb{C}_{33}b_1 + \mathbb{C}_{34}b_2 = 0,\\ &\mathbb{C}_{41}a_1 + \mathbb{C}_{42}a_2 + \mathbb{C}_{43}b_1 + \mathbb{C}_{44}b_2 = 0 \end{aligned} \tag{56}$$

with respect to a_i and b_i $(i = 1, 2)$, where coefficients $\mathbb{C}_{ij}$ $(i, j = 1, \ldots, 4)$ are functions of the hydrodynamic coefficients $\mathtt{d}_\mathtt{i}$ and $\mathtt{g}_\mathtt{j}$ of the original nonlinear modal equations system as well as of $\bar\lambda$ $(\bar\lambda = \lambda/\sigma)$ and the amplitude parameters A_1 and B_2 of the generalized coordinates $p_1(t)$ and $r_1(t)$ whose expressions are given by formulae (B.3).

Requiring a non-trivial solution of (56) with respect to a_i and b_i $(i = 1, 2)$ leads to the zero-determinant condition

$$\mathbf{D}(\lambda) = \begin{vmatrix} \mathbb{C}_{11} & \mathbb{C}_{12} & \mathbb{C}_{13} & \mathbb{C}_{14} \\ \mathbb{C}_{21} & \mathbb{C}_{22} & \mathbb{C}_{13} & \mathbb{C}_{24} \\ \mathbb{C}_{31} & \mathbb{C}_{32} & \mathbb{C}_{33} & \mathbb{C}_{34} \\ \mathbb{C}_{41} & \mathbb{C}_{42} & \mathbb{C}_{43} & \mathbb{C}_{44} \end{vmatrix} = 0 \tag{57}$$

whose roots are the required characteristic exponents $\bar\lambda$.

8. The response curves

Figures 9 and 10 present the response curves (in terms of the amplitude parameters A_1 and B_2) associated with the steady-state wave motions. Accounting for the secondary resonance analysis in section 6 and the related limitations of the Moiseev-type modal equations, the focus is on the semi-apex angles $\theta_0 = 30^\circ$ and 45° and the ratios $\mathtt{r}_1 = 0.5$ and 0.4, respectively.

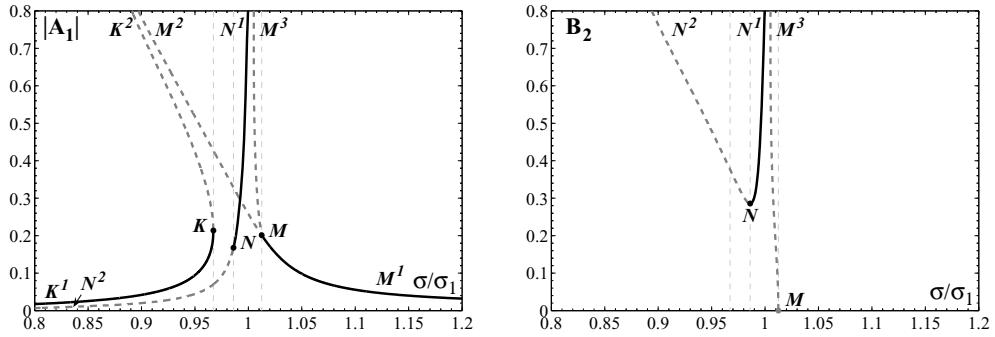

Figure 10. The same as in figure 9 but for $\theta_0 = 45^\circ$, $\mathtt{r}_1 = 0.4$ and $H = 0.01$.

Analyzing the response curves makes it possible to estimate the effective frequency ranges for planar and/or swirling sloshing. The amplitude parameter A_1 measures the longitudinal wave component but B_2 corresponds to the cross-wave component. The solid lines mark stable steady-state wave regimes but dashed lines are used to denote their instability.

The figures demonstrate that the response curves are qualitatively similar to those known for non-truncated conical tanks Gavrilyuk *et al* (2005). *Firstly*, the planar sloshing (branches $K^1\,K^2$ and M^1M^2) is always unstable in a neighborhood of the linear resonance ($\sigma/\sigma_1 = 1$); the instability is expected for the forcing frequencies laying between the abscissas of K and M. Here, K is the turning point but M is the Poincaré bifurcation point from which the branch MM^3 corresponding to unstable swirling emerges. *Secondly*, stable swirling exists at $\sigma/\sigma_1 = 1$. The 'swirling' branch, N^2N^1, is divided by the Hopf bifurcation point N so that subbranch NN^1 corresponds to stable steady-state wave motions (the abscissa of N is less than 1) but the subbranch NN^2 implies unstable steady-state swirling. *Thirdly*, the interval between the abscissas of N and M marks the frequency range where both planar and swirling steady-state wave regimes are unstable. In this frequency range, irregular (chaotic) waves are expected.

The literature on experimental studies devoted to nonlinear resonant sloshing in a truncated conical tank is almost empty. Being interested in these experiments to validate our theoretical results, we paid attention to Casciati *et al* (2003) where appropriate experiments were mentioned in the context of the tuned liquid dampers equipped with a conical tank. Thanks to Professor Fabio Casciati and Dr Emiliano Matta (Politecnico di Torino, Italy), we have got a more detailed report on these experiments documented in the PhD Thesis by Matta (2002). In the Thesis, the experimental tank with the semi-apex angle $\theta_0 = 30^\circ$ was used for measuring the hydrodynamic force occurring due to a horizontal harmonic tank excitation. The thesis reports a set of the hydrodynamic force recordings as well as trying to classify the liquid motions based on both measurements and observations. Because the experimental series were conducted on a relatively short time scale, the classification was only partly successful. In some cases, it was possible to conclude on almost steady-state wave regime (planar or swirling), but many of the Matta's experimental series reported strong breaking waves and irregular motions which may be explained as either continuing transients or hydrodynamic instability. However, these irregular and almost steady-state liquid motions were found as they follow from our analysis: irregular waves were established for $\sigma/\sigma_1 < 1$, a few stable model series demonstrated swirling for $\sigma/\sigma_1 > 1$ and stable planar waves were detected far from the linear resonance $\sigma/\sigma_1 = 1$. This qualitatively supports our theory. As for a quantitative validation, we think that it is difficult to do because the experimental series were relatively

short in the time. Moreover, the experiments were done with relatively small (almost shallow) liquid depths causing the ratio $\mathtt{r}_1 = 0.852$. Section 6 shows that, unfortunately, this ratio is too close to $\mathtt{r}_1 = 0.8926$ (the secondary resonance by the mode (0,1)) and $\mathtt{r}_1 = 0.835$ (the secondary resonance by the mode (3,2)). This means that the Moiseev type modal equations are most likely inapplicable to this shallow water sloshing to get a quantitative agreement due to these secondary resonances. The secondary resonances are implicitly confirmed in observations of Matta (2002). Breaking waves and overturning are almost always detected for the forcing frequencies in a neighborhood of $\sigma/\sigma_1 = 1$ where our theory predicts irregular waves or swirling. As was discussed in chapters 8 and 9 by Faltinsen and Timokha (2009), these phenomena are a typical attribute of multiple secondary resonances, especially, for the shallow water case.

9. Conclusions

Employing the non-conformal mapping technique by Lukovsky (1990) and the Moiseev-type asymptotics, we derived approximate weakly nonlinear modal equations which describe resonant liquid sloshing in the V-shaped truncated conical tank. The modal system couples seven generalized coordinates of the considered infinite-dimensional mechanical system. The generalized coordinates are associated with perturbations of the seven lowest natural sloshing modes. The considered weakly nonlinear resonant sloshing is assumed to be due to a small-magnitude excitation of the lowest natural sloshing frequency and there are no secondary resonances amplifying higher generalized coordinates. Arguments in choosing the seven generalized coordinates (see section 4.3) are based on physical circumstances and referring to earlier successful nonlinear modal systems for an upright circular cylindrical tank.

Along with ideas and derivation details, the present paper presents the numerical non-dimensional hydrodynamic coefficients which can be useful for practically oriented readers. We studied the limit cases to ensure that there are no algebraic and arithmetic errors.

Using the nonlinear Moiseev-type modal equations, we studied the resonant steady-state sloshing occurring due to harmonic tank excitations with the forcing frequency close to the lowest natural sloshing frequency. Combining the Bubnov–Galerkin and asymptotic schemes, we constructed a time-periodic solution of the nonlinear modal equations and, using the first Lyapunov method, studied stability of this solution.

Physically, the time-periodic solution yields two types of steady-state wave motions, planar and swirling. The planar sloshing implies liquid motions in the excitation plane but swirling means a rotary wave. The response curves were drawn to show a similarity between the steady-state sloshing in truncated conical tanks and upright circular cylindrical tanks. Qualitative agreement was found with experimental observations on steady-state wave motions by Matta (2002).

Acknowledgment

The authors acknowledge the financial support of the German Research Council (DFG).

Appendix A. Technical details of derivations

The employed natural sloshing modes are $\varphi_1 = \psi_0$, $\varphi_2 = \sin x_3\psi_1$, $\varphi_3 = \cos x_3\psi_1$, $\varphi_4 = \sin 2x_3\psi_2$, $\varphi_5 = \cos 2x_3\psi_2$, $\varphi_6 = \sin 3x_3\psi_2$, $\varphi_7 = \cos 3x_3\psi_2$ that implies $f(x_2, x_3) = \beta_0 + f_0(x_2)p_0 + f_1(x_2)p_1\cos x_3 + f_1(x_2)r_1\sin x_3 + f_2(x_2)p_2\cos 2x_3 + f_2(x_2)r_2\sin 2x_3 + f_3(x_2)p_3 \times$

$\cos 3x_3 + f_3(x_2)r_3 \sin 3x_3$ in (26) where the time-dependent function $\beta_0(t)$ follows from the volume conservation condition

$$\int_0^{2\pi}\int_0^{x_{20}} x_2\left(x_{10}^2 f + x_{10} f^2 + \frac{1}{3}f^3\right)\mathrm{d}x_2\,\mathrm{d}x_3 = 0$$

and takes (neglecting the higher-order terms) the form $\beta_0 = k_1 p_0^2 + k_2(p_1^2 + r_1^2) + k_3 p_0(r_1^2 + p_1^2) + k_4(2p_1r_1r_2 - p_2(r_1^2 + p_1^2)) + k_5(p_2^2 + r_2^2) + k_6(p_3^2 + r_3^2) + k_7(p_1r_2r_3 + p_1p_2p_3 - r_1r_2p_3 + r_1p_2r_3) + \cdots$. The coefficients k_i are computed by the formulae

$$k_1 = -\frac{2e_{00}}{h_t x_{20}^2},\quad k_2 = -\frac{e_{11}}{x_{20}^2 h_t},\quad k_3 = -\frac{e_{011}}{h_t^2 x_{20}^2},\quad k_4 = -\frac{e_{112}}{2h_t^2 x_{20}^2},\quad k_5 = -\frac{e_{22}}{h_t x_{20}^2},$$

$$k_6 = -\frac{e_{33}}{h_t x_{20}^2},\quad k_7 = -\frac{e_{123}}{h_t^2 x_{20}^2},\quad k_8 = \frac{\pi}{4}\left(h_t^4 - h_b^4\right)x_{20}^2,\quad k_9 = \frac{\pi}{2}h_t^2 e_{11},\quad k_{10} = \pi h_t^2 e_{00},$$

$$k_{11} = \frac{\pi}{2}h_t^2 e_{22},\quad k_{12} = \frac{\pi}{2}h_t^2 e_{33},\quad k_{13} = 2\pi h_t e_{011},\quad k_{14} = \pi h_t e_{112},\quad k_{15} = 2\pi h_t e_{123},$$

$$k_{16} = \frac{3\pi}{2}\left(\frac{e_{1111}}{8} - \frac{e_{11}^2}{x_{20}^2}\right),\quad k_{17} = \frac{\pi}{4}e_{1113},$$

where $h_t = h_1 = \mathtt{r}_1\cot\theta_0$, $h_b = h_0 = \mathtt{r}_0\cot\theta_0$ and $e_{ijk} = \int_0^{x_{20}} x_2 f_i(x_2) f_j(x_2) f_k(x_2)\mathrm{d}x_2$.

The vector (l_1, l_2, l_3) by (14) reads as

$$l_1 = \rho\int_0^{2\pi}\int_0^{x_{20}}\int_{h_b}^{f+h_t} x_1^3 x_2\,\mathrm{d}x_1\,\mathrm{d}x_2\,\mathrm{d}x_3,\quad l_2 = \rho\int_0^{2\pi}\int_0^{x_{20}}\int_{h_b}^{f+h_t} x_1^3 x_2^2\cos x_3\,\mathrm{d}x_1\,\mathrm{d}x_2\,\mathrm{d}x_3,$$

$$l_3 = \rho\int_0^{2\pi}\int_0^{x_{20}}\int_{h_b}^{f+h_t} x_1^3 x_2^2\sin x_3\,\mathrm{d}x_1\,\mathrm{d}x_2\,\mathrm{d}x_3$$

and takes the form

$$l_1 = \lambda_{10} + \lambda_{11}\left(p_1^2 + r_1^2\right) + \cdots, \tag{A.1}$$

$$l_2 = \lambda_{21}p_1 + \lambda_{22}p_1\left(p_1^2 + r_1^2\right) + \lambda_{23}p_0p_1 + \lambda_{24}\left(p_1p_2 + r_1r_2\right) + \cdots, \tag{A.2}$$

$$l_3 = \lambda_{31}r_1 + \lambda_{32}r_1\left(p_1^2 + r_1^2\right) + \lambda_{33}p_0r_1 + \lambda_{34}\left(p_1r_2 - p_2r_1\right) + \cdots, \tag{A.3}$$

where $\lambda_{10} = k_8$, $\lambda_{11} = k_9$, $\lambda = \lambda_{21} = \lambda_{31} = \lambda_{i1}$, $\lambda_{22} = \lambda_{32} = \lambda_{i2}$, $\lambda_{23} = \lambda_{33} = \lambda_{i3}$ and $\lambda_{24} = \lambda_{34} = \lambda_{i4}$, are computed by the formulae $\lambda_{i1} = \pi\rho h_t^3 s_{0100}^2$, $\lambda_{i2} = \frac{3\pi\rho h_t}{4x_{20}^2}\left(x_{20}^2 s_{0300}^2 - 4s_{0200}^1 s_{0100}^2\right)$, $\lambda_{i3} = 3\pi\rho h_t^2 s_{1100}^2$, $\lambda_{i4} = \frac{3}{2}\pi\rho h_t^2 s_{0110}^2$, $s_{0200}^1 = e_{11}$, and quadratures s_{ijkl}^2 $(i, j, k, l = 0, 1, 2, 3)$ are defined by

$$s_{ijkl}^2 = \int_0^{x_{20}} x_2^2 (f_0(x_2))^i (f_1(x_2))^j (f_2(x_2))^k (f_3(x_2))^l\,\mathrm{d}x_2,$$

where the coefficients i, j, k, l mean the power of functions $f_m(x_2)$. Coefficients λ_{ijk} are given by the formulae $\lambda_{211} = \lambda_{311} = \lambda_{i1}$, $\lambda_{2131} = \lambda_{3131} = \frac{1}{4}(3\lambda_{i2} - (4o_0^{(0)} + o_0^{(2)})\lambda_{i3} - (4o_2^{(0)} + o_2^{(2)})\lambda_{i4})$, $\lambda_{2132} = \lambda_{3132} = \frac{1}{4}(\lambda_{i2} - (4o_0^{(0)} - o_0^{(2)})\lambda_{i3} + (4o_2^{(0)} - 3o_2^{(2)})\lambda_{i4})$, $\lambda_{233} = \lambda_{333} = \frac{9}{4}(\lambda_{i2} - o_0^{(2)}\lambda_{i3} - o_2^{(2)}\lambda_{i4})$.

Explicit representation of (A.1) appearing in (13) takes the form $l_1 = k_8 + k_9(p_1^2 + r_1^2) + k_{10}p_0^2 + k_{11}(p_2^2 + r_2^2) + k_{12}(p_3^2 + r_3^2) + k_{14}(2p_1r_1r_2 + p_2(p_1^2 - r_1^2)) + k_{13}p_0(r_1^2 + p_1^2) + k_{16}(2p_1^2r_1^2 + p_1^4 + r_1^4) + k_{15}(r_1(p_2r_3 - p_3r_2) + p_1(r_2r_3 + p_2p_3)) + k_{17}(p_1p_3(p_1^2 - 3r_1^2) + r_1r_3(3p_1^2 - r_1^2))$.

Within the introduced seven generalized coordinates, the asymptotic expansion of (14) leads to

$$A_1 = b_1 + b_2 p_0 + b_3(p_1^2 + r_1^2) + b_4 p_0^2 + b_5(r_2^2 + p_2^2) + b_6 p_0(p_1^2 + r_1^2) + b_7(p_1^2 p_2 + 2p_1 r_1 r_2 - p_2 r_1^2),$$

$$A_2 = b_8 r_1 + b_9 r_1(p_1^2 + r_1^2) + b_{11} p_0 r_1 + b_{10}(p_1 r_2 - r_1 p_2) + b_{12}(p_2 r_3 - r_2 p_3) + b_{13}(r_3(p_1^2 - r_1^2) - 2p_1 r_1 p_3),$$

$$A_3 = b_8 p_1 + b_9 p_1(p_1^2 + r_1^2) + b_{11} p_0 p_1 + b_{10}(p_1 p_2 + r_1 r_2) + b_{12}(p_2 p_3 + r_2 r_3) + b_{13}(p_3(p_1^2 - r_1^2) + 2p_1 r_1 r_3),$$

$$A_4 = b_{14} r_2 + 2b_{15} p_1 r_1 + b_{16} p_0 r_2 + 2b_{19} p_0 p_1 r_1 + b_{17} r_2(p_1^2 + r_1^2) + b_{18}(p_1 r_3 - p_3 r_1),$$

$$A_5 = b_{14} p_2 + b_{15}(p_1^2 - r_1^2) + b_{16} p_0 p_2 + b_{17} p_2(p_1^2 + r_1^2) + b_{18}(p_1 p_3 + r_1 r_3) + b_{19} p_0(p_1^2 - r_1^2),$$

$$A_6 = b_{20} r_3 + b_{21} r_1(3p_1^2 - r_1^2) + b_{24} p_0 r_3 + b_{22}(r_1 p_2 + p_1 r_2) + b_{23} r_3(p_1^2 + r_1^2),$$

$$A_7 = b_{20} p_3 + b_{21} p_1(p_1^2 - 3r_1^2) + b_{24} p_0 p_3 + b_{22}(p_1 p_2 - r_1 r_2) + b_{23} p_3(p_1^2 + r_1^2),$$

$$A_{11} = b_{25} + b_{26} p_0 + b_{27}(p_1^2 + r_1^2),$$

$$A_{12} = b_{28} r_1 + b_{29} p_0 r_1 + b_{30}(p_1 r_2 - r_1 p_2) + b_{31} r_1(p_1^2 + r_1^2),$$

$$A_{13} = b_{28} p_1 + b_{29} p_0 p_1 + b_{30}(p_1 p_2 + r_1 r_2) + b_{31} p_1(p_1^2 + r_1^2),$$

$$A_{14} = b_{32} r_2 + 2b_{33} p_1 r_1 + b_{34}(p_1 r_3 - r_1 p_3),$$

$$A_{15} = b_{32} p_2 + b_{33}(p_1^2 - r_1^2) + b_{34}(p_1 p_3 + r_1 r_3),$$

$$A_{16} = b_{35} r_3 + b_{36}(p_1 r_2 + r_1 p_2),$$

$$A_{17} = b_{35} p_3 + b_{36}(p_1 p_2 - r_1 r_2),$$

$$A_{22} = b_{37} + b_{38} p_0 + b_{39} p_2 + b_{40} p_1^2 + b_{41} r_1^2 + b_{42}(p_1 p_3 + r_1 r_3),$$

$$A_{23} = -b_{39} r_2 + b_{43} p_1 r_1 + b_{42}(r_1 p_3 - p_1 r_3),$$

$$A_{24} = b_{44} p_1 + b_{45} p_3 + b_{46} p_0 p_1 + b_{47} p_1 p_2 + b_{48} r_1 r_2 + b_{49} p_1(p_1^2 + r_1^2),$$

$$A_{25} = -b_{44} r_1 - b_{45} r_3 - b_{46} p_0 r_1 - b_{47} p_1 r_2 + b_{48} r_1 p_2 - b_{49} r_1(p_1^2 + r_1^2),$$

$$A_{26} = b_{50} p_2 + b_{51}(p_1^2 - r_1^2) + b_{52} p_1 p_3 + b_{53} r_1 r_3,$$

$$A_{27} = -b_{50} r_2 - 2b_{51} p_1 r_1 - b_{52} p_1 r_3 + b_{53} r_1 p_3,$$

$$A_{33} = b_{37} + b_{38} p_0 - b_{39} p_2 + b_{40} r_1^2 + b_{41} p_1^2 - b_{42}(p_1 p_3 + r_1 r_3),$$

$$A_{34} = b_{44} r_1 - b_{45} r_3 + b_{46} p_0 r_1 - b_{47} r_1 p_2 + b_{48} p_1 r_2 + b_{49} r_1(p_1^2 + r_1^2),$$

$$A_{35} = b_{44} p_1 - b_{45} p_3 + b_{46} p_0 p_1 + b_{47} r_1 r_2 + b_{48} p_1 p_2 + b_{49} p_1(p_1^2 + r_1^2),$$

$$A_{36} = b_{50} r_2 + 2b_{51} p_1 r_1 - b_{52} r_1 p_3 + b_{53} p_1 r_3,$$

$$A_{37} = b_{50} p_2 + b_{51}(p_1^2 - r_1^2) + b_{52} r_1 r_3 + b_{53} p_1 p_3,$$

$$A_{44} = b_{54} + b_{55} p_0 + b_{56}(p_1^2 + r_1^2) + b_{57}(p_1 p_3 - r_1 r_3),$$

$$A_{45} = -b_{57}(r_1 p_3 + p_1 r_3), \quad A_{67} = 0,$$

$$A_{46} = b_{58} p_1 + b_{59} p_0 p_1 + b_{60}(p_1 p_2 + r_1 r_2) + b_{61} p_1(p_1^2 + r_1^2),$$

$$A_{47} = -b_{58} r_1 - b_{59} p_0 r_1 + b_{60}(r_1 p_2 - p_1 r_2) + b_{61} r_1(r_1^2 - p_1^2),$$

$$A_{55} = b_{54} + b_{55} p_0 + b_{56}(p_1^2 + r_1^2) + b_{57}(r_1 r_3 - p_1 p_3),$$

$$A_{56} = b_{58} r_1 + b_{59} p_0 r_1 + b_{60}(p_1 r_2 - r_1 p_2) + b_{61} r_1 (p_1^2 + r_1^2),$$
$$A_{57} = b_{58} p_1 + b_{59} p_0 p_1 + b_{60}(p_1 p_2 + r_1 r_2) + b_{61} p_1 (p_1^2 + r_1^2),$$
$$A_{66} = b_{62} + b_{63} p_0 + b_{64}(p_1^2 + r_1^2),$$
$$A_{77} = b_{62} + b_{63} p_0 + b_{64}(p_1^2 + r_1^2).$$

Considering (12) as a system of linear equations with respect to the generalized velocities gives the asymptotic solution

$$P_0 = c_1 \dot{p}_0 + c_2 p_1 \dot{p}_1 + c_2 r_1 \dot{r}_1,$$
$$R_1 = c_3 \dot{r}_1 + c_4 r_1 \dot{p}_0 + c_5 p_0 \dot{r}_1 + c_6 p_1 \dot{r}_2 - c_6 r_1 \dot{p}_2 + c_7 r_2 \dot{p}_1 - c_7 p_2 \dot{r}_1 + c_8 p_1 r_1 \dot{p}_1 + c_9 r_1^2 \dot{r}_1 + c_{10} p_1^2 \dot{r}_1,$$
$$P_1 = c_3 \dot{p}_1 + c_4 p_1 \dot{p}_0 + c_5 p_0 \dot{p}_1 + c_6 p_1 \dot{p}_2 + c_6 r_1 \dot{r}_2 + c_7 p_2 \dot{p}_1 + c_7 r_2 \dot{r}_1 + c_8 p_1 r_1 \dot{r}_1 + c_9 p_1^2 \dot{p}_1 + c_{10} r_1^2 \dot{p}_1,$$
$$R_2 = c_{11} \dot{r}_2 + c_{12} r_1 \dot{p}_1 + c_{12} p_1 \dot{r}_1, \quad P_2 = c_{11} \dot{p}_2 + c_{12} p_1 \dot{p}_1 - c_{12} r_1 \dot{r}_1,$$
$$R_3 = c_{13} \dot{r}_3 + c_{14} p_1 \dot{r}_2 + c_{14} r_1 \dot{p}_2 + c_{15} p_2 \dot{r}_1 + c_{15} r_2 \dot{p}_1 + c_{16} p_1^2 \dot{r}_1 + 2 c_{16} p_1 r_1 \dot{p}_1 - c_{16} r_1^2 \dot{r}_1,$$
$$P_3 = c_{13} \dot{p}_3 + c_{14} p_1 \dot{p}_2 - c_{14} r_1 \dot{r}_2 + c_{15} p_2 \dot{p}_1 - c_{15} r_2 \dot{r}_1 + c_{16} p_1^2 \dot{p}_1 - 2 c_{16} p_1 r_1 \dot{r}_1 - c_{16} r_1^2 \dot{p}_1,$$

where

$$c_1 = \frac{b_2}{b_{25}}, \quad c_2 = \frac{1}{b_{25}} \left(2 b_3 - \frac{b_8 b_{28}}{b_{37}} \right), \quad c_3 = \frac{b_8}{b_{37}}, \quad c_4 = \frac{1}{b_{37}} \left(b_{11} - \frac{b_2 b_{28}}{b_{25}} \right),$$

$$c_5 = \frac{1}{b_{37}} \left(b_{11} - \frac{b_8 b_{38}}{b_{37}} \right), \quad c_6 = \frac{1}{b_{37}} \left(b_{10} - \frac{b_{14} b_{44}}{b_{54}} \right), \quad c_7 = \frac{1}{b_{37}} \left(b_{10} - \frac{b_8 b_{39}}{b_{37}} \right),$$

$$c_8 = \frac{1}{b_{37}} \left(2 \left(b_9 - \frac{b_3 b_{28}}{b_{25}} \right) - \frac{b_8}{b_{37}} \left(b_{43} - \frac{b_{28}^2}{b_{25}} \right) \right),$$

$$c_9 = \frac{1}{b_{37}} \left(3 b_9 - \frac{2 b_{28}}{b_{25}} \left(b_3 - \frac{b_8 b_{28}}{b_{37}} \right) - \frac{b_8}{b_{37}} \left(b_{41} + \frac{b_{28}^2}{b_{25}} \right) - \frac{b_{44}}{b_{54}} \left(2 b_{15} - \frac{b_8 b_{44}}{b_{37}} \right) \right),$$

$$c_{10} = \frac{1}{b_{37}} \left(b_9 - \frac{2 b_{15} b_{44}}{b_{54}} - \frac{b_8}{b_{37}} \left(b_{40} - \frac{b_{44}^2}{b_{54}} \right) \right), \quad c_{15} = \frac{1}{b_{62}} \left(b_{22} - \frac{b_8 b_{50}}{b_{37}} \right),$$

$$c_{11} = \frac{b_{14}}{b_{54}}, \quad c_{12} = \frac{1}{b_{54}} \left(2 b_{15} - \frac{b_8 b_{44}}{b_{37}} \right), \quad c_{13} = \frac{b_{20}}{b_{62}}, \quad c_{14} = \frac{1}{b_{62}} \left(b_{22} - \frac{b_{14} b_{58}}{b_{54}} \right),$$

$$c_{16} = \frac{1}{b_{62}} \left(3 b_{21} - \frac{b_8}{b_{37}} \left(b_{51} + \frac{b_{44} b_{58}}{b_{54}} \right) - \frac{2 b_{58}}{b_{54}} \left(b_{15} - \frac{b_8 b_{44}}{b_{37}} \right) \right)$$

in which b_i $(i = 1, \ldots, 64)$ are expressed by the following formulae $b_1 = 2 g_{00}$, $b_3 = g_{0211} + 2 k_2 g_{01}$, $b_2 = 2 g_{010}$, $b_4 = 2 g_{0200} + 2 k_1 g_{01}$, $b_5 = g_{0222} + 2 k_5 g_{01}$, $b_6 = 3 g_{03011} + 4 k_2 g_{020} + 2 k_3 g_{01}$,

$b_7 = \frac{3}{2}g_{03112} + 2\,k_4\,g_{01}$, $b_8 = g_{111}$, $b_{10} = g_{1212}$, $b_9 = \frac{3}{4}g_{13111} + 2k_2 g_{121}$, $b_{11} = 2g_{1201}$, $b_{12} = g_{1223}$, $b_{13} = \frac{3}{4}g_{13113}$, $b_{14} = g_{212}$, $b_{15} = \frac{1}{2}g_{2211}$, $b_{16} = 2g_{2202}$, $b_{17} = \frac{3}{2}g_{23112} + 2k_2 g_{222}$, $b_{18} = g_{2213}$, $b_{19} = \frac{3}{2}g_{23011}$, $b_{20} = g_{313}$, $b_{21} = \frac{1}{4}g_{33111}$, $b_{22} = g_{3212}$, $b_{23} = \frac{3}{2}g_{33113} + 2k_2 g_{323}$, $b_{24} = 2g_{3203}$, $b_{25} = 2q_{000}$, $b_{26} = 2q_{0010}$, $b_{28} = q_{0111}$, $b_{27} = q_{00211} + 2k_2 q_{001}$, $b_{29} = 2q_{01201}$, $b_{30} = q_{01212}$, $b_{31} = 2k_2 q_{0121}$, $b_{32} = q_{0212}$, $b_{33} = \frac{1}{2}q_{02211}$, $b_{34} = q_{02213}$, $b_{35} = q_{0313}$, $b_{36} = q_{03212}$, $b_{37} = q_{110}$, $b_{38} = q_{1110}$, $b_{39} = \frac{1}{2}q_{1112}$, $b_{40} = k_2 q_{111} + \frac{1}{4}q_{112111}$, $b_{41} = k_2 q_{111} + \frac{1}{4}q_{112112}$, $b_{42} = \frac{1}{2}q_{11213}$, $b_{43} = \frac{1}{2}q_{11211}$, $b_{44} = q_{1211}$, $b_{45} = q_{1213}$, $b_{46} = q_{12201}$, $b_{47} = 2q_{122121}$, $b_{48} = q_{122122}$, $b_{49} = k_2 q_{1221}$, $b_{50} = \frac{1}{2}q_{1312}$, $b_{51} = \frac{1}{4}q_{13211}$, $b_{52} = 3q_{132131}$, $b_{53} = q_{132132}$, $b_{54} = q_{220}$, $b_{55} = q_{2210}$, $b_{56} = k_2\,q_{221} + q_{22211}$, $b_{57} = q_{22213}$, $b_{58} = q_{2311}$, $b_{59} = q_{23201}$, $b_{60} = q_{23212}$, $b_{61} = k_2\,q_{2321}$, $b_{62} = q_{330}$, $b_{63} = q_{3310}$, $b_{64} = k_2\,q_{331} + q_{33211}$ with quadratures

$$g_{ikjln} = \pi \int_0^{x_{20}} x_2 B_k^i(x_2)\, f_j(x_2)\, f_l(x_2)\, f_n(x_2)\, \mathrm{d}x_2$$

and $q_{000} = q_{000}^f$, $q_{0111} = q_{0111}^f$, $q_{110} = q_{110}^b + q_{110}^f$, $q_{1110} = q_{1110}^b + q_{1110}^f$, $q_{1112} = q_{1112}^b - q_{1112}^f$, $q_{111} = q_{111}^b + q_{111}^f$, $q_{11213} = q_{11213}^b - q_{11213}^f$, $q_{112111} = 3\,q_{11211}^b + q_{11211}^f$, $q_{112112} = q_{11211}^b + 3q_{11211}^f$, $q_{1211} = q_{1211}^b + q_{1211}^f/2$, $q_{1213} = q_{1213}^b - q_{1213}^f/2$, $q_{1312} = 3\,q_{1312}^b + q_{1312}^f$, $q_{13211} = 3\,q_{13211}^b + q_{13211}^f$, $q_{220} = 4\,q_{220}^b + q_{220}^f 4$, $q_{2311} = 3\,q_{2311}^b + q_{2311}^f/2$, $q_{330} = 9\,q_{330}^b + q_{330}^f$ within

$$q_{ijkln}^b = \pi \int_0^{x_{20}} \frac{B_k^{ij}(x_2)}{x_2} f_l(x_2)\, f_n(x_2)\, \mathrm{d}x_2, \quad q_{ijkln}^f = \pi \int_0^{x_{20}} F_k^{ij}(x_2)\, f_l(x_2)\, f_n(x_2)\, \mathrm{d}x_2.$$

Here, the integrands $F_k^{ij}(x_2)$, $B_k^{ij}(x_2)$ and $B_k^i(x_2)$ depend on $b_k^{(m)}(x_2)$ and $\bar{b}_k^{(m)}(x_2)$:

$$F_i^{nk}(x_2) = x_2 D_i^{nk} - x_2^2(E_i^{nk} - E_i^{kn}) + x_2(1 + x_2^2)C_i^{nk},$$

$$B_i^m(x_2) = \sum_{k=0}^{q_1} s_i^1 b_k^m + \sum_{n=0}^{q_2} s_i^2 \bar{b}_n^m, \quad i = 0, \ldots, 3, \quad B_l^{nk} = X_{l,0}^{nk}(b_i^n, b_j^k),$$

where

$$X_{l,l_k}^{nk}(x, y) = k_l \left(\sum_{i=l_k}^{q_1} \sum_{j=l_k}^{q_1} s_l^{11} x y + \sum_{i=l_k}^{q_1} \sum_{j=l_k}^{q_2} s_l^{12} x \bar{y} + \sum_{i=l_k}^{q_2} \sum_{j=l_k}^{q_1} s_l^{21} \bar{x} y + \sum_{i=l_k}^{q_2} \sum_{j=l_k}^{q_2} s_l^{22} \bar{x} \bar{y} \right),$$

$$k_l = \begin{cases} 1, & l = 0, 1, \\ 1/2, & l = 2, \end{cases} \qquad l_k = 0, 1$$

within

$$s_0^{11} = \frac{h_t^{1+\nu_{ni}+\nu_{kj}} - h_b^{1+\nu_{ni}+\nu_{kj}}}{1 + \nu_{ni} + \nu_{kj}}, \quad s_0^{12} = \frac{h_t^{\nu_{ni}-\nu_{kj}} - h_b^{\nu_{ni}-\nu_{kj}}}{\nu_{ni} - \nu_{kj}}, \quad s_0^{21} = \frac{h_t^{\nu_{kj}-\nu_{ni}} - h_b^{\nu_{kj}-\nu_{ni}}}{\nu_{kj} - \nu_{ni}},$$

$$s_0^{22} = \frac{h_t^{-1-\nu_{ni}-\nu_{kj}} - h_b^{-1-\nu_{ni}-\nu_{kj}}}{-1 - \nu_{ni} - \nu_{kj}}, \quad s_1^{11} = h_t^{\nu_{ni}+\nu_{kj}}, \quad s_1^{12} = h_t^{-1+\nu_{ni}-\nu_{kj}}, \quad s_1^{21} = h_t^{-1-\nu_{ni}+\nu_{kj}},$$

$$s_1^{22} = h_t^{-2-\nu_{ni}-\nu_{kj}}, \quad s_2^{11} = h_t^{-1+\nu_{ni}+\nu_{kj}}(\nu_{ni} + \nu_{kj}), \quad s_2^{12} = h_t^{-2+\nu_{ni}-\nu_{kj}}(\nu_{ni} - \nu_{kj} - 1),$$

$$s_2^{21}=h_t^{-2-\nu_{ni}+\nu_{kj}}(\nu_{kj}-\nu_{ni}-1),\quad s_2^{22}=h_t^{-3-\nu_{ni}-\nu_{kj}}(\nu_{ni}+\nu_{kj}+2),\quad s_0^1=\frac{h_t^{\nu_{mk}+3}-h_b^{\nu_{mk}+3}}{\nu_{mk}+3},$$

$$s_1^1=h_t^{\nu_{mk}+2},\quad s_0^2=\frac{h_t^{2-\nu_{mn}}-h_b^{2-\nu_{mn}}}{2-\nu_{mn}},\quad s_1^2=h_t^{1-\nu_{mn}},\quad s_2^1=\frac{1}{2}h_t^{\nu_{mk}+1}(\nu_{mk}+2),$$

$$s_2^2=\frac{1-\nu_{mn}}{2h_t^{\nu_{mn}}},\quad s_3^1=\frac{1}{6}h_t^{\nu_{mk}}(\nu_{mk}+1)(\nu_{mk}+2),\quad s_3^2=\frac{1}{6}h_t^{-\nu_{mn}-1}(\nu_{mn}-1)\nu_{mn},$$

$$C_l^{nk}=X_{l,1}^{nk}(c_i^n,c_j^k),\quad D_l^{nk}=X_{l,1}^{nk}(d_i^n,d_j^k),\quad E_l^{nk}=X_{l,1}^{nk}(d_i^n,c_j^k),\quad E_l^{kn}=X_{l,1}^{nk}(c_i^n,d_j^k)$$

provided by $d_i^n=\nu_{ni}b_i^n$, $d_j^k=\nu_{kj}b_j^k$, $\bar d_i^n=(-1-\nu_{ni})\bar b_i^n$, $\bar d_j^k=(-1-\nu_{kj})\bar b_j^k$ and

$$c_i^n=\frac{\partial b_i^n}{\partial x_2},\quad \bar c_i^n=\frac{\partial \bar b_i^n}{\partial x_2},\quad c_j^k=\frac{\partial b_j^k}{\partial x_2},\quad \bar c_j^k=\frac{\partial \bar b_j^k}{\partial x_2}.$$

Functions $b_k^{(m)}(x_2)=a_{1k}^{(m)}v_{\nu_{mk}}^{(m)}(x_2)$, $\bar b_k^{(m)}(x_2)=\bar a_{1k}^{(m)}\bar v_{\nu_{mk}}^{(m)}(x_2)$, $m=0,1,2,3$ are taken from expansion of the surface natural sloshing modes

$$f_m(x_2)=a_{10}^{(m)}+\sum_{k=1}^{q_1}b_k^{(m)}(x_2)+\bar a_{10}^{(m)}+\sum_{k=1}^{q_1}\bar b_k^{(m)}(x_2)\quad (m=0,1,2,3)$$

provided by $a_{10}^{(0)}\neq 0$, $\bar a_{10}^{(0)}\neq 0$, $v_{\nu_{00}}^{(0)}=\bar v_{\nu_{00}}^{(0)}=1$, $a_{10}^{(i)}=\bar a_{10}^{(i)}=0$, $i=1,2,3$, where the natural sloshing modes read as

$$\psi_{mn}(x_1,x_2)=\sum_{k=0}^{q_1}x_1{}^{\nu_{mk}}b_{\nu_{mk}}^{(m)}(x_2)+\sum_{k=0}^{q_2}x_1{}^{-1-\nu_{mk}}\bar b_{\nu_{mk}}^{(m)}(x_2)$$

and $a_{nk}^{(m)}=\hat a_{nk}^{(m)}/N_{mn}$, $\bar a_{nk}^{(m)}=\hat{\bar a}_{nk}^{(m)}/N_{mn}$, is the normalization based on $N_{mn}=\psi_{mn}(x_{10},x_{20})=1$. A detailed definition of the functions $v_{\nu_{mk}}^{(m)}(x_2)$ and $\bar v_{\nu_{mk}}^{(m)}(x_2)$ was given by Gavrilyuk *et al* (2005).

The non-dimensional hydrodynamic coefficients $\mathtt{d}_i$ and $\mathtt{g}_j$ $(m=0,1,2,3,i=1,\dots,15,j=0,\dots,6)$ follow after substituting the above expressions in the dynamic equations and neglecting the higher-order terms than $O(\epsilon)$. This gives

$$\mathtt{d}_1=\frac{d_1}{\mu_1},\quad \mathtt{d}_2=\frac{d_2}{\mu_1},\quad \mathtt{d}_3=\frac{d_3}{\mu_1},\quad \mathtt{d}_4=\frac{d_4}{\mu_1},\quad \mathtt{d}_5=\frac{d_5}{\mu_1},\quad \mathtt{d}_6=\frac{d_6}{\mu_1},\quad \mathtt{d}_7=\frac{d_7}{\mu_2},$$
$$\mathtt{d}_8=\frac{d_8}{\mu_0},\quad \mathtt{d}_9=\frac{d_9}{\mu_2},\quad \mathtt{d}_{10}=\frac{d_{10}}{\mu_0},\quad \mathtt{d}_{11}=\frac{d_{11}}{\mu_3},\quad \mathtt{d}_{12}=\frac{d_{12}}{\mu_3},\quad \mathtt{d}_{13}=\frac{d_{13}}{\mu_3},\quad \mathtt{d}_{14}=\frac{d_{14}}{\mu_3},$$
$$\mathtt{d}_{15}=\frac{d_{15}}{\mu_3},\quad \mathtt{g}_0=\frac{k_{13}}{\kappa_{01}\mu_0},\quad \mathtt{g}_1=\frac{2k_{13}}{\kappa_{11}\mu_1},\quad \mathtt{g}_2=\frac{2k_{14}}{\kappa_{11}\mu_1},\quad \mathtt{g}_3=\frac{4k_{16}}{\kappa_{11}\mu_1},\quad \mathtt{g}_4=\frac{k_{14}}{\kappa_{21}\mu_2},$$
$$\mathtt{g}_5=\frac{k_{15}}{\kappa_{31}\mu_3},\quad \mathtt{g}_6=\frac{k_{17}}{\kappa_{31}\mu_3},$$

where $\Lambda=\lambda/\mu_1$ and

$$\mu_0=b_2c_1,\quad \mu_1=b_8c_3,\quad \mu_2=b_{14}c_{11},\quad \mu_3=b_{20}c_{13},$$
$$d_2=b_9c_3+b_8c_{10}+2b_{15}c_{12},\quad d_1=2b_3c_2+3b_9c_3+b_8c_9+2b_{15}c_{12},$$
$$d_2=b_9c_3+b_8c_{10}+2b_{15}c_{12},\quad d_3=b_{10}c_3+b_8c_7,\quad d_4=b_8c_6+2b_{15}c_{11},\quad d_5=b_{11}c_3+b_8c_5,$$

$d_6 = 2b_3c_1 + b_8c_4, \quad d_7 = b_{14}c_{12} - \frac{1}{2}(b_{39}c_3^2), \quad d_8 = b_2c_2 + \frac{1}{2}(b_{38}c_3^2), \quad d_9 = b_{10}c_3 + b_{14}c_{12},$

$d_{10} = b_2c_2 + b_{11}c_3, \quad d_{12} = b_{18}c_{12} - \frac{1}{2}(b_{42}c_3^2) - b_{45}c_3c_{12} + 2b_{20}c_{16}, \quad d_{13} = b_{12}c_3 + b_{20}c_{15},$

$d_{14} = b_{18}c_{11} + b_{20}c_{14}, \quad d_{15} = -b_{45}c_3c_{11} + b_{20}c_{14} + b_{20}c_{15}, \quad d_{11} = b_{13}c_3 + b_{18}c_{12} + b_{20}c_{16}.$

Appendix B. Important expressions

Coefficients of the algebraic system (44) take the form

$$m_1 = -\frac{\mathtt{d}_1}{2} + \mathtt{d}_3\left(o_2^{(0)} - \frac{1}{4}o_2^{(2)}\right) + \mathtt{d}_4 o_2^{(2)} + \mathtt{d}_5\left(o_0^{(0)} - \frac{1}{4}o_0^{(2)}\right) + \mathtt{d}_6 o_0^{(2)}$$
$$+ \left[\frac{3}{4}\mathtt{g}_3 - \mathtt{g}_1\left(o_0^{(0)} + \frac{1}{4}o_0^{(2)}\right) - \mathtt{g}_2\left(o_2^{(0)} + \frac{1}{4}o_2^{(2)}\right)\right]\bar\sigma_1^2,$$

$$m_3 = m_1 - m_2,$$

$$m_2 = \frac{1}{2}\mathtt{d}_1 - 2\mathtt{d}_2 - \mathtt{d}_3\left(o_2^{(0)} + \frac{3}{4}o_2^{(2)}\right) + 3\mathtt{d}_4 o_2^{(2)} + \mathtt{d}_5\left(o_0^{(0)} + \frac{1}{4}o_0^{(2)}\right) - \mathtt{d}_6 o_0^{(2)}$$
$$+ \left[\frac{1}{4}\mathtt{g}_3 - \mathtt{g}_1\left(o_0^{(0)} - \frac{1}{4}o_0^{(2)}\right) + \mathtt{g}_2\left(o_2^{(0)} - \frac{3}{4}o_2^{(2)}\right)\right]\bar\sigma_1^2,$$

$$m_4 = m_1 + m_2. \tag{B.1}$$

The values o_m^k appearing in expressions for the periodic solution are

$$o_0^{(0)} = \frac{\mathtt{d}_8 - \mathtt{d}_{10} + \mathtt{g}_0\,\bar\sigma_0^2}{2\,\bar\sigma_0^2}, \quad o_0^{(2)} = \frac{\mathtt{d}_8 + \mathtt{d}_{10} - \mathtt{g}_0\,\bar\sigma_0^2}{4 - \bar\sigma_0^2},$$

$$o_2^{(0)} = \frac{\mathtt{d}_7 - \mathtt{d}_9 + \mathtt{g}_4\,\bar\sigma_2^2}{2\,\bar\sigma_2^2}, \quad o_2^{(2)} = \frac{\mathtt{d}_7 + \mathtt{d}_9 - \mathtt{g}_4\,\bar\sigma_2^2}{4 - \bar\sigma_2^2},$$

$$o_3^{(1)} = \frac{1}{4(1-\bar\sigma_3^2)}(3\,\mathtt{d}_{11} - \mathtt{d}_{12} - 4\,\mathtt{d}_{13}o_2^{(0)} - (\mathtt{d}_{13} + 4\,\mathtt{d}_{14} - 2\,\mathtt{d}_{15})o_2^{(2)}$$
$$-(3\mathtt{g}_6 - \mathtt{g}_5(4\,o_2^{(0)} + o_2^{(2)})\bar\sigma_3^2)), \quad \bar\sigma_i^2 = \frac{\sigma_i^2}{\sigma^2}, \quad i = 0, 1, 2, 3,$$

$$o_3^{(3)} = \frac{1}{4(9-\bar\sigma_3^2)}(\mathtt{d}_{11} + \mathtt{d}_{12} - (\mathtt{d}_{13} + 4\,\mathtt{d}_{14} + 2\,\mathtt{d}_{15})o_2^{(2)} - (\mathtt{g}_6 - \mathtt{g}_5\,o_2^{(2)})\bar\sigma_3^2). \tag{B.2}$$

Coefficients $\mathbb{C}_{ij}$ $(i, j = 1, \ldots, 4)$ of the linear algebraic system (56) are expressed in terms of $\mathtt{d}_i$ and $\mathtt{g}_j$, $\bar\lambda$ ($\bar\lambda = \lambda/\sigma$) and the amplitude parameters A_1 and B_2

$$\begin{array}{llll}
\mathbb{C}_{11} = A_1^2C_7 + B_2^2C_8 + C_{14}, & \mathbb{C}_{12} = A_1^2C_1 + B_2^2C_2 + C_{13}, & \mathbb{C}_{13} = A_1B_2C_5, & \\
\mathbb{C}_{14} = A_1B_2C_9, & \mathbb{C}_{21} = A_1^2C_3 + B_2^2C_4 - C_{13}, & \mathbb{C}_{22} = A_1^2C_{10} + B_2^2C_{11} + C_{14}, & \\
\mathbb{C}_{23} = A_1B_2C_{12}, & \mathbb{C}_{24} = A_1B_2C_6, & \mathbb{C}_{31} = -A_1B_2C_6, & \mathbb{C}_{32} = A_1B_2C_{12}, \\
\mathbb{C}_{33} = A_1^2C_{11} + B_2^2C_{10} + C_{14}, & \mathbb{C}_{34} = -A_1^2C_4 - B_2^2C_3 + C_{13}, & \mathbb{C}_{41} = A_1B_2C_9, & \\
\mathbb{C}_{42} = -A_1B_2C_5, & \mathbb{C}_{43} = -A_1^2C_2 - B_2^2C_1 - C_{13}, & \mathbb{C}_{44} = A_1^2C_8 + B_2^2C_7 + C_{14}. &
\end{array} \tag{B.3}$$

Coefficients C_i of (B.3) are defined as follows:

$$C_1 = \gamma_0^{(1)}\delta_1^{(1)} - \tfrac{1}{2}\gamma_0^{(3)}\delta_1^{(2)} - \gamma_2^{(1)}\delta_2^{(1)} - \tfrac{1}{2}\gamma_2^{(3)}\delta_2^{(2)} + \bar\lambda(\mathtt{d}_1 - 2\delta_0^{(3^+)} + \tfrac{1}{2}\mathtt{d}_{56}\gamma_0^{(4)} + \tfrac{1}{2}\mathtt{d}_{34}\gamma_2^{(4)}),$$

$$C_2 = \bar\lambda(\mathtt{d}_2 - 2\delta_0^{(3^-)} - \mathtt{d}_3\gamma_2^{(2)} + \tfrac{1}{2}\mathtt{d}_{34}\gamma_2^{(4)}) - \tfrac{1}{2}\gamma_2^{(3)}\delta_2^{(2)},$$

$$C_3 = \tfrac{1}{2}\gamma_0^{(3)}\delta_1^{(2)} + \tfrac{1}{2}\gamma_2^{(3)}\delta_2^{(2)} + \bar{\lambda}(-\mathtt{d}_1 + 2\delta_0^{(3^+)} + \mathtt{d}_5\gamma_0^{(2)} - \tfrac{1}{2}\mathtt{d}_{56}\gamma_0^{(4)} - \mathtt{d}_3\gamma_2^{(2)} - \tfrac{1}{2}\mathtt{d}_{34}\gamma_2^{(4)}),$$

$$C_4 = -\gamma_2^{(1)}\delta_2^{(1)} + \tfrac{1}{2}\gamma_2^{(3)}\delta_2^{(2)} + \bar{\lambda}(-\mathtt{d}_2 + 2\delta_0^{(3^-)} - \tfrac{1}{2}\mathtt{d}_{34}\gamma_2^{(4)}),$$

$$C_5 = -\gamma_0^{(1)}\delta_1^{(1)} - \tfrac{1}{2}\gamma_0^{(3)}\delta_1^{(2)} - \gamma_2^{(1)}\delta_2^{(1)} + \gamma_2^{(3)}\delta_2^{(2)} + \bar{\lambda}(\mathtt{d}_1 - 3\mathtt{d}_2 - \mathtt{d}_3\gamma_2^{(2)} + \tfrac{1}{2}\mathtt{d}_{56}\gamma_0^{(4)} - \mathtt{d}_{34}\gamma_2^{(4)}),$$

$$C_6 = -\tfrac{1}{2}\gamma_0^{(3)}\delta_1^{(2)} + \gamma_2^{(1)}\delta_2^{(1)} + \gamma_2^{(3)}\delta_2^{(2)} + \bar{\lambda}(\mathtt{d}_1 - 3\mathtt{d}_2 + \mathtt{d}_5\gamma_0^{(2)} + d_3\gamma_2^{(2)} + \tfrac{1}{2}\mathtt{d}_{56}\gamma_0^{(4)} - \mathtt{d}_{34}\gamma_2^{(4)}),$$

$$\begin{aligned} C_7 = {} & \tfrac{3}{4}(\bar{\lambda}^2 - 2)\mathtt{d}_1 - (\bar{\lambda}^2 - 1)\mathtt{d}_5 o_0^{(0)} - (\bar{\lambda}^2 - 1)\mathtt{d}_3 o_2^{(0)} - \tfrac{1}{4}o_0^{(2)}\delta_1^{(0)} - \gamma_0^{(2)}\delta_1^{(1)} - \tfrac{1}{2}\gamma_0^{(4)}\delta_1^{(2)} \\ & - \tfrac{1}{4}o_2^{(2)}\delta_2^{(0)} + \gamma_2^{(2)}\delta_2^{(1)} - \tfrac{1}{2}\gamma_2^{(4)}\delta_2^{(2)} - \tfrac{1}{2}\bar{\lambda}(\mathtt{d}_{56}\gamma_0^{(3)} + \mathtt{d}_{34}\gamma_2^{(3)}) \\ & + \tfrac{1}{4}\bar{\sigma}_1^2(9g_3 - \mathtt{g}_1\delta_0^{(0^+)} - \mathtt{g}_2\delta_0^{(2^+)}), \end{aligned}$$

$$\begin{aligned} C_8 = {} & \tfrac{1}{2}d_1 + \tfrac{1}{4}(\bar{\lambda}^2 - 8)\mathtt{d}_2 + \tfrac{1}{4}o_0^{(2)}\delta_1^{(0)} - (\bar{\lambda}^2 - 1)\mathtt{d}_5 o_0^{(0)} + (\bar{\lambda}^2 - 1)\mathtt{d}_3 o_2^{(0)} - \tfrac{1}{4}o_2^{(2)}\delta_2^{(0)} \\ & - \tfrac{1}{2}\gamma_2^{(4)}\delta_2^{(2)} - \bar{\lambda}(\mathtt{d}_3\gamma_2^{(1)} + \tfrac{1}{2}\mathtt{d}_{34}\gamma_2^{(3)}) + \tfrac{1}{4}\bar{\sigma}_1^2(\mathtt{g}_3 - \mathtt{g}_1\delta_0^{(0^-)} + \mathtt{g}_2\delta_0^{(2^-)}), \end{aligned}$$

$$\begin{aligned} C_9 = {} & \tfrac{1}{4}(\bar{\lambda}^2 + 4)\mathtt{d}_1 - \tfrac{1}{4}(\bar{\lambda}^2 + 16)\mathtt{d}_2 - \gamma_0^{(2)}\delta_1^{(1)} + \tfrac{1}{2}\gamma_0^{(4)}\delta_1^{(2)} - \tfrac{1}{4}o_2^{(2)}\delta_2^{(0)} - \gamma_2^{(2)}\delta_2^{(1)} - \gamma_2^{(4)}\delta_2^{(2)} \\ & + \bar{\lambda}(\tfrac{1}{2}\mathtt{d}_{56}\gamma_0^{(3)} + \mathtt{d}_3\gamma_2^{(1)} - \mathtt{d}_{34}\gamma_2^{(3)}) + \tfrac{1}{2}\bar{\sigma}_1^2(\mathtt{g}_3 - \mathtt{g}_2 o_2^{(2)}), \end{aligned}$$

$$\begin{aligned} C_{10} = {} & \tfrac{1}{4}(\bar{\lambda}^2 - 2)\mathtt{d}_1 - (\bar{\lambda}^2 - 1)\mathtt{d}_5 o_0^{(0)} - (\bar{\lambda}^2 - 1)\mathtt{d}_3 o_2^{(0)} + \tfrac{1}{4}o_0^{(2)}\delta_1^{(0)} - \tfrac{1}{2}\gamma_0^{(4)}\delta_1^{(2)} + \tfrac{1}{4}o_2^{(2)}\delta_2^{(0)} \\ & - \tfrac{1}{2}\gamma_2^{(4)}\delta_2^{(2)} - \tfrac{1}{2}\bar{\lambda}(2\mathtt{d}_5\gamma_0^{(1)} + \mathtt{d}_{56}\gamma_0^{(3)} - 2\mathtt{d}_3\gamma_2^{(1)} + \mathtt{d}_{34}\gamma_2^{(3)}) \\ & + \tfrac{1}{4}\bar{\sigma}_1^2(3g_3 - \mathtt{g}_1\delta_0^{(0^-)} - \mathtt{g}_2\delta_0^{(2^-)}), \end{aligned}$$

$$\begin{aligned} C_{11} = {} & -\tfrac{1}{2}d_1 + \tfrac{3}{4}\bar{\lambda}^2\mathtt{d}_2 - (\bar{\lambda}^2 - 1)\mathtt{d}_5 o_0^{(0)} + (\bar{\lambda}^2 - 1)\mathtt{d}_3 o_2^{(0)} - \tfrac{1}{4}o_0^{(2)}\delta_1^{(0)} + \tfrac{1}{4}o_2^{(2)}\delta_2^{(0)} - \gamma_2^{(2)}\delta_2^{(1)} \\ & - \tfrac{1}{2}\gamma_2^{(4)}\delta_2^{(2)} - \tfrac{1}{2}\bar{\lambda}\mathtt{d}_{34}\gamma_2^{(3)} + \tfrac{1}{4}\bar{\sigma}_1^2(3g_3 - \mathtt{g}_1\delta_0^{(0^+)} + \mathtt{g}_2\delta_0^{(2^+)}), \end{aligned}$$

$$\begin{aligned} C_{12} = {} & \tfrac{1}{4}(\bar{\lambda}^2 - 4)\mathtt{d}_1 - \tfrac{1}{4}(\bar{\lambda}^2 - 8)\mathtt{d}_2 - \gamma_2^{(2)}\delta_2^{(1)} + \gamma_2^{(4)}\delta_2^{(2)} - \tfrac{1}{2}\gamma_0^{(4)}\delta_1^{(2)} - \tfrac{1}{4}o_2^{(2)}\delta_2^{(0)} \\ & + \bar{\lambda}(\mathtt{d}_5\gamma_0^{(1)} - \tfrac{1}{2}\mathtt{d}_{56}\gamma_0^{(3)} + \mathtt{d}_3\gamma_2^{(1)} + \mathtt{d}_{34}\gamma_2^{(3)}) + \tfrac{1}{2}\bar{\sigma}_1^2(\mathtt{g}_3 - \mathtt{g}_2 o_2^{(2)}), \end{aligned}$$

$$C_{13} = 2\bar{\lambda}, \quad C_{14} = \bar{\lambda}^2 + \bar{\sigma}_1^2 - 1.$$

Here we introduce (use) the following notations:

$$\delta_0^{(0^-)} = 4o_0^{(0)} - o_0^{(2)}, \quad \delta_0^{(2^-)} = 4o_2^{(0)} - o_2^{(2)}, \quad \delta_0^{(3^-)} = \mathtt{d}_5 o_0^{(0)} - \mathtt{d}_3 o_2^{(0)}, \quad \mathtt{d}_{34} = \mathtt{d}_3 - 4\mathtt{d}_4,$$

$$\delta_0^{(0^+)} = 4o_0^{(0)} + o_0^{(2)}, \quad \delta_0^{(2^+)} = 4o_2^{(0)} + o_2^{(2)}, \quad \delta_0^{(3^+)} = \mathtt{d}_5 o_0^{(0)} + \mathtt{d}_3 o_2^{(0)}, \quad \mathtt{d}_{56} = \mathtt{d}_5 - 4\mathtt{d}_6,$$

$$\delta_1^{(0)} = \bar{\lambda}^2\mathtt{d}_5 + \mathtt{d}_{56}, \quad \delta_1^{(1)} = \bar{\lambda}^2\mathtt{d}_6 + \mathtt{g}_1\bar{\sigma}_1^2 - \mathtt{d}_5, \quad \delta_1^{(2)} = \bar{\lambda}^2\mathtt{d}_6 + \mathtt{g}_1\bar{\sigma}_1^2 + \mathtt{d}_{56},$$

$$\delta_2^{(0)} = \bar{\lambda}^2\mathtt{d}_3 + \mathtt{d}_{34}, \quad \delta_2^{(1)} = \bar{\lambda}^2\mathtt{d}_4 + \mathtt{g}_2\bar{\sigma}_1^2 - \mathtt{d}_3, \quad \delta_2^{(2)} = \bar{\lambda}^2\mathtt{d}_4 + \mathtt{g}_2\bar{\sigma}_1^2 + \mathtt{d}_{34}.$$

References

Bridges T 1986 *SIAM J. App. Math.* **47** 40–59
Bridges T 1987 *J. Fluid Mech.* **179** 137–53
Casciati F, Stefano A D and Matta E 2003 *Simul. Modelling Pract. Theory* **11** 353–70
Faltinsen O and Timokha A 2009 *Sloshing* (Cambridge: University Press Cambridge)
Faltinsen O and Timokha A 2013 *J. Fluid Mech.* **719** 129–64
Faltinsen O, Rognebakke O, Lukovsky I and Timokha A 2000 *J. Fluid Mech.* **407** 201–34
Faltinsen O, Rognebakke O and Timokha A 2006 *Phys. Fluids* **18** 012103
Faltinsen O, Firoozkoohi R and Timokha A 2011 *Phys. Fluids* **23** 062106
Gavrilyuk I, Lukovsky I, Trotsenko Y and Timokha A 2007 *J. Eng. Math.* **57** 57–78
Gavrilyuk I, Hermann M, Lukovsky I, Solodun O and Timokha A 2008 *Eng. Comput.* **25** 518–40
Gavrilyuk I, Hermann M, Lukovsky I, Solodun O and Timokha A 2012 *Eng. Comput.* **29** 198–220
Gavrilyuk I P, Lukovsky I A and Timokha A N 2005 *Fluid Dyn. Res.* **37** 399–429
Ikeda T and Ibrahim R 2005 *J. Sound Vib.* **284** 75–102
Ikeda T, Ibrahim R, Harata Y and Kuriyama T 2012 *J. Fluid Mech.* **700** 304–28
La Rocca M, Scortino M and Boniforti M 2000 *Fluid Dyn. Res.* **27** 225–9
Limarchenko O 2007 *Ukr. Math. J.* **59** 45–69
Love J and Tait M 2010 *J. Fluids Struct.* **26** 1058–77
Love J and Tait M 2011 *Int. J. Non-Linear Mech.* **46** 1065–75
Love J, Tait M and Toopchi-Nezhad H 2011 *Eng. Struct.* **33** 738–46
Lukovsky I 1975 *Nonlinear Sloshing in Tanks of Complex Geometrical Shape* (Kiev: Naukova Dumka) (in Russian)
Lukovsky I 1990 *Introduction to Nonlinear Dynamics of Rigid Bodies With the Cavities Partially Filled by a Fluid* (Kiev: Naukova Dumka) (in Russian)
Lukovsky I and Timokha A 1995 *Variational Methods in Nonlinear Problems of the Dynamics of a Limited Liquid Volume* (Kiev: Institute of Mathematics of NASU) (in Russian)
Lukovsky I and Timokha A 2002 *Int. J. Fluid Mech. Res.* **29** 216–42
Lukovsky I, Ovchynnykov D and Timokha A 2012 *Nonlinear Oscillations* **14** 512–25
Matta E 2002 Sistemi di attenuazione della risposta dinamica a massa oscillante solida e fluida *PhD Thesis* Politecnico di Torino, Torino
Moiseev N N 1958 *J. Appl. Math. Mech.* **22** 860–72
Moore R and Perko L 1964 *J. Fluid Mech.* **22** 305–20
Narimanov G 1957 *Prikl. Mat. Mekh.* **21** 513–24
Ockendon J and Ockendon H 1973 *J. Fluid Mech.* **59** 397–413
Ockendon J R, Ockendon H and Waterhouse D D 1996 *J. Fluid Mech.* **315** 317–44
Perko L 1969 *J. Fluid Mech.* **35** 77–96
Takahara H and Kimura K 2012 *J. Sound Vib.* **331** 3199–212
Waterhouse D 1994 *J. Fluid Mech.* **281** 313–8